A detailed life history of a pleistocene steppe bison (Bison priscus) skeleton unearthed in Arctic Alaska

Article *in* Quaternary Science Reviews · October 2020

DOI: 10.1016/j.quascirev.2020.106578

CITATION
1

READS
603

9 authors, including:

Juliette Funck
University of Alaska Fairbanks
3 PUBLICATIONS **5** CITATIONS
SEE PROFILE

Peter D Heintzman
UiT The Arctic University of Norway
59 PUBLICATIONS **1,179** CITATIONS
SEE PROFILE

Gemma G R Murray
University of Cambridge
23 PUBLICATIONS **490** CITATIONS
SEE PROFILE

Beth Shapiro
University of California, Santa Cruz
507 PUBLICATIONS **17,018** CITATIONS
SEE PROFILE

Quaternary Science Reviews 249 (2020) 106578

Contents lists available at ScienceDirect

Quaternary Science Reviews

journal homepage: www.elsevier.com/locate/quascirev

A detailed life history of a pleistocene steppe bison (*Bison priscus*) skeleton unearthed in Arctic Alaska

Juliette Funck [a, b, **], Peter D. Heintzman [c, d], Gemma G.R. Murray [e], Beth Shapiro [c, f], Holly McKinney [g], Jean-Bernard Huchet [h], Nancy Bigelow [i], Patrick Druckenmiller [b, j], Matthew J. Wooller [a, k, *]

[a] *Alaska Stable Isotope Facility, Water and Environmental Research Center, Institute of Northern Engineering, University of Alaska Fairbanks, Fairbanks, AK, 99775, USA*
[b] *Department of Geosciences, University of Alaska Fairbanks, Fairbanks, AK, 99775, USA*
[c] *Department of Ecology and Evolutionary Biology, University of California Santa Cruz, Santa Cruz, CA, 95064, USA*
[d] *The Arctic University Museum of Norway, UiT - the Arctic University of Norway, NO-9037, Tromsø, Norway*
[e] *Department of Veterinary Medicine, University of Cambridge, Cambridge, CB3 0ES, UK*
[f] *Howard Hughes Medical Institute, University of California Santa Cruz, Santa Cruz, CA, 95064, USA*
[g] *Department of Anthropology, University of Alaska Fairbanks, Fairbanks, AK, 99775, USA*
[h] *Muséum National d'Histoire Naturelle, Institut de Systématique, Evolution, Biodiversité (ISYEB), Unit Mixte de Recherche 7205, CP50, Entomologie, 45, Rue Buffon, F-75005, Paris, France*
[i] *Alaska Quaternary Center, University of Alaska Fairbanks, Fairbanks, AK, 99775, USA*
[j] *University of Alaska, Fairbanks, University of Alaska Fairbanks, AK, 99775, USA*
[k] *College of Fisheries and Ocean Sciences, University of Alaska Fairbanks, Fairbanks, AK, 99775, USA*

ARTICLE INFO

Article history:
Received 12 November 2019
Received in revised form
10 August 2020
Accepted 1 September 2020
Available online xxx

Keywords:
Quaternary
Beringia
Paleoecology
Stable isotopes
Strontium
Oxygen
Carbon
Nitrogen
Steppe bison

ABSTRACT

Detailed paleoecological evidence from Arctic Alaska's past megafauna can help reconstruct paleoenvironmental conditions and can illustrate ecological adaptation to varying environments. We examined a rare, largely articulated and almost complete skeleton of a steppe bison (*Bison priscus*) recently unearthed in Northern Alaska. We used a multi-proxy paleoecological approach to reconstruct the past ecology of an individual representing a key ancient taxon. Radiocarbon dating of horn keratin revealed that the specimen has a finite radiocarbon age ~46,000 ± 1000 cal yr BP, very close to the limit of radiocarbon dating. We also employed Bayesian age modeling of the mitochondrial genome, which estimated an age of ~33,000–87,000 cal yr BP. Our taphonomic investigations show that the bison was scavenged post-mortem and infested by blowflies before burial. Stable carbon and oxygen isotope ($\delta^{13}C$ and $\delta^{15}N$) analyses of sequentially sampled horn keratin reveal a seasonal cycle; furthermore, high $\delta^{15}N$ values during its first few years of life are consistent with patterns observed in modern bison that undertook dispersal. We compared sequential analyses of tooth enamel for strontium isotope ratios ($^{87}Sr/^{86}Sr$) to a spatial model of $^{87}Sr/^{86}Sr$ values providing evidence for dispersal across the landscape. Synthesis of the paleoecological findings indicates the specimen lived during interstadial conditions. Our multi-proxy, paleoecological approach, combining light and heavy isotope ratios along with genetic information, adds to the broader understanding of ancient bison ecology during the Late Pleistocene, indicating that ancient bison adopted different degrees of paleo-mobility according to the prevailing paleoecological conditions and climate.

1. Introduction

1.1. Paleoecological context

Northern Alaska is currently experiencing environmental changes as the result of global warming, which is occurring most

* Corresponding author. Alaska Stable Isotope Facility, Water and Environmental Research Center, Institute of Northern Engineering, University of Alaska Fairbanks, Fairbanks, AK, 99775, USA.
** Corresponding author. Alaska Stable Isotope Facility, Water and Environmental Research Center, Institute of Northern Engineering, University of Alaska Fairbanks, Fairbanks, AK, 99775, USA.
E-mail addresses: jmfunck@alaska.edu (J. Funck), mjwooller@alaska.edu (M.J. Wooller).

https://doi.org/10.1016/j.quascirev.2020.106578
0277-3791/

rapidly at northern latitudes (Moon et al., 2019). These changes impact the mobility and ecologies of extant megafauna including caribou, moose, and muskoxen (Post and Forchhammer, 2008; Sharma et al., 2009). For example, migratory species are experiencing mismatch in timing of migration and peak resource availability (Post and Forchhammer, 2008), while caribou are losing habitat in the north due to warmer Arctic summers and winters (Sharma et al., 2009). Detailed paleoecological evidence from the remains of past megafauna from this region provides an opportunity to examine how past megafauna lived in this environment (Guthrie, 1989), and therefore help predict responses of living megafauna to present and projected environmental changes.

During the height of the last glaciation (~28–18 thousand years ago (kya)) (Clark et al., 2009), the North Slope of Alaska was part of an expansive land-mass known as Beringia. Sea levels were ~130 m lower than today (Lambeck et al., 2014), exposing a shallow continental shelf between northeast Asia and North America known as the Bering Land Bridge (BLB). The BLB extended approximately from the Lena River, Russia, in the west and the Mackenzie River, Yukon, Canada, in the east (Elias and Crocker, 2008) (Fig. 1). The Beringian ecosystem was primarily that of a mammoth steppe, a graminoid-dominated ecosystem that supported a community of large herbivorous mammals, dominated by mammoths (*Mamamuthus primigenius*), horses (*Equus* sp.), and steppe bison (*Bison priscus*) (Guthrie, 2001; Mann et al., 2013; Shapiro and Cooper, 2003; Zimov et al., 2012). The mammoth steppe supported large populations of these herbivores, many of which had larger body sizes than their descendants today at similar latitudes (Zimov et al., 2012). Bison, in particular, had larger body sizes and horns than present-day American bison (*Bison bison*) (Martin et al., 2018), and were present throughout most of Eurasia and North America in what has been termed "The Bison Belt" (Guthrie, 1989). Steppe bison first arrived in North America ~195–135 kya (Froese et al., 2017) and their population began to decline around 37 kya (Heintzman et al., 2016; Shapiro et al., 2004).

Modern bison ecology can provide an analog for inferring ancient bison behavior as well as the basis for comparative (paleo) biology and anatomy. Although modern plains bison (*Bison bison bison*) are often considered grassland grazing specialists (Bamforth, 1987), plains bison in northern habitats (Waggoner and Hinkes, 1986), wood bison (*Bison bison athabascae*) (Larter and Gates, 1991), and european wisents (*Bison bonasus*) have been observed to regularly utilize browse in their diet (Kowalczyk et al., 2011). Evidence from macro and micro tooth-wear analysis indicates that steppe bison likely had a broader herbivorous diet and ecological niche that included browsing (Rivals et al., 2010, 2007; Saarinen et al., 2016). The long-distance (>100 km) (Berger, 2004; Hanson, 2015; Plumb et al., 2009) migrations of American bison (*Bison bison*) across the American Great Plains were legendary and a key component of bison life history (Bamforth, 1987; Flores, 1991). However, isotopic (strontium) analyses of ancient (~18,500 ^{14}C yr BP) bison (*Bison priscus*) from a site in Ukraine found no evidence of paleomobility (Julien et al., 2012). Analyses of ancient bison specimens can provide opportunities to flesh out the paleoecological life-history of a taxon that shaped Beringian ecosystems (Zimov et al., 2011).

Fortunately for paleoecologists, bones, teeth, and horns of bison are some of the most numerous fossil remains found in Alaska (Guthrie, 1970; Mann et al., 2013). On rare occasions, high sediment deposition rates along with freezing temperatures can result in preservation of virtually complete carcasses or skeletons of past Beringian fauna, revealing vivid paleoecological snap-shots of life in Beringia (Boeskorov et al., 2016; Kirillova et al., 2015; Van Geel et al., 2014; Zazula et al., 2009, 2017). These rare and well-preserved glimpses of past megafaunal paleoecology can emerge from eroding river-banks (Mann et al., 2013; Zazula et al., 2009), during mining operations (Guthrie, 1968), and during construction activities (Zazula et al., 2017). In some instances, soft tissue such as hair, skin, organs, and stomach contents are preserved (Kirillova et al., 2015; Van Geel et al., 2014), as well as associated insects. These remains, along with bones and teeth, can retain chemical clues about an individual's paleoecology. Isotopic analyses (Kirillova et al., 2015) and analyses of ancient DNA (aDNA) (Zazula et al., 2017) can reveal past mobility patterns and population interconnectivity, contributing to an understanding of past ecosystems, landscapes, and evolution (Froese et al., 2017; Haile et al., 2009; Marsolier-Kergoat et al., 2015; Shapiro and Cooper, 2003; Heintzman et al., 2016; Shapiro et al., 2004).

In this study, we conducted a multi-proxy study, combining isotopic and aDNA analyses, with supporting paleo-forensic analyses, to investigate the sex, age, paleoecology and life history of an exceptionally well-preserved and largely articulated steppe bison (*Bison priscus*) found on the North Slope of Alaska (Fig. 1 a-c). We further assess peri- and post-mortem events together with the taphonomic history of skeletal remains using a taphonomic analysis of the skeleton and of the plant and insect remains present. Our examination of the physical condition of the remains (bones and teeth) from the specimen provides clues about an individual's age, sex, and appearance (Fuller, 1959). The taphonomy and geology associated with the specimen provides information about the context surrounding an organism's death and a possible cause of death. We used insect (Elias et al., 2000) and plant (Bigelow et al., 2013) macrofossils associated with the bison's remains to provide valuable paleoecological information. Our multi-proxy, paleoecological approach adds to the broader understanding of ancient bison ecology during the Late Pleistocene.

1.2. Stable isotopes

Isotopic analyses have become a popular tool in paleoecology for determining the ecological and life-history traits of ancient fauna (Bocherens, 2003; Britton et al., 2009). Tissues that form in discrete layers over a period of an individual's life, such as tooth enamel, hair, or horn, can be subsampled to allow inference of inter- and intra-annual paleo-mobility and paleoecology using isotopic analyses of these sample types (Balasse et al., 2001; Britton et al., 2009; Stevens et al., 2011; Zazzo et al., 2012). Intra-tooth strontium isotope ratio (^{87}Sr/^{86}Sr) analysis has been developed as a useful tool to track the mobility of past animals and humans (Balasse, 2002; Britton, 2009; Britton et al., 2011; Hoppe et al., 1999; Hoppe, 2004; Julien et al., 2012; Koch et al., 1995; Pellegrini et al., 2008; Radloff et al., 2010; Viner et al., 2010; Widga et al., 2010). ^{87}Sr/^{86}Sr ratios can vary across landscapes depending in part on the age and rock type of the underlying geology (Bataille et al., 2014; Brennan et al., 2014). These landscape ^{87}Sr/^{86}Sr signatures can enter animals through their diet and drinking water, replacing calcium in tissues such as teeth and bones (Capo et al., 1998). The combination of ^{87}Sr/^{86}Sr and oxygen isotopic (δ^{18}O) values from analyses of animal tissues have proved to be a powerful predictor of geographic location (Britton et al., 2009; Gigleux et al., 2017; Knudson et al., 2009). The δ^{18}O values from a specimen can indicate location based on latitude and distance from the coast (Hoppe, 2006; Lachniet et al., 2016). The δ^{18}O values from analyses of bison teeth have also been used to determine approximate local climate and seasonal temperature variation, because δ^{18}O values in water can be closely related to temperature (Bernard et al., 2009; Hoppe et al.,

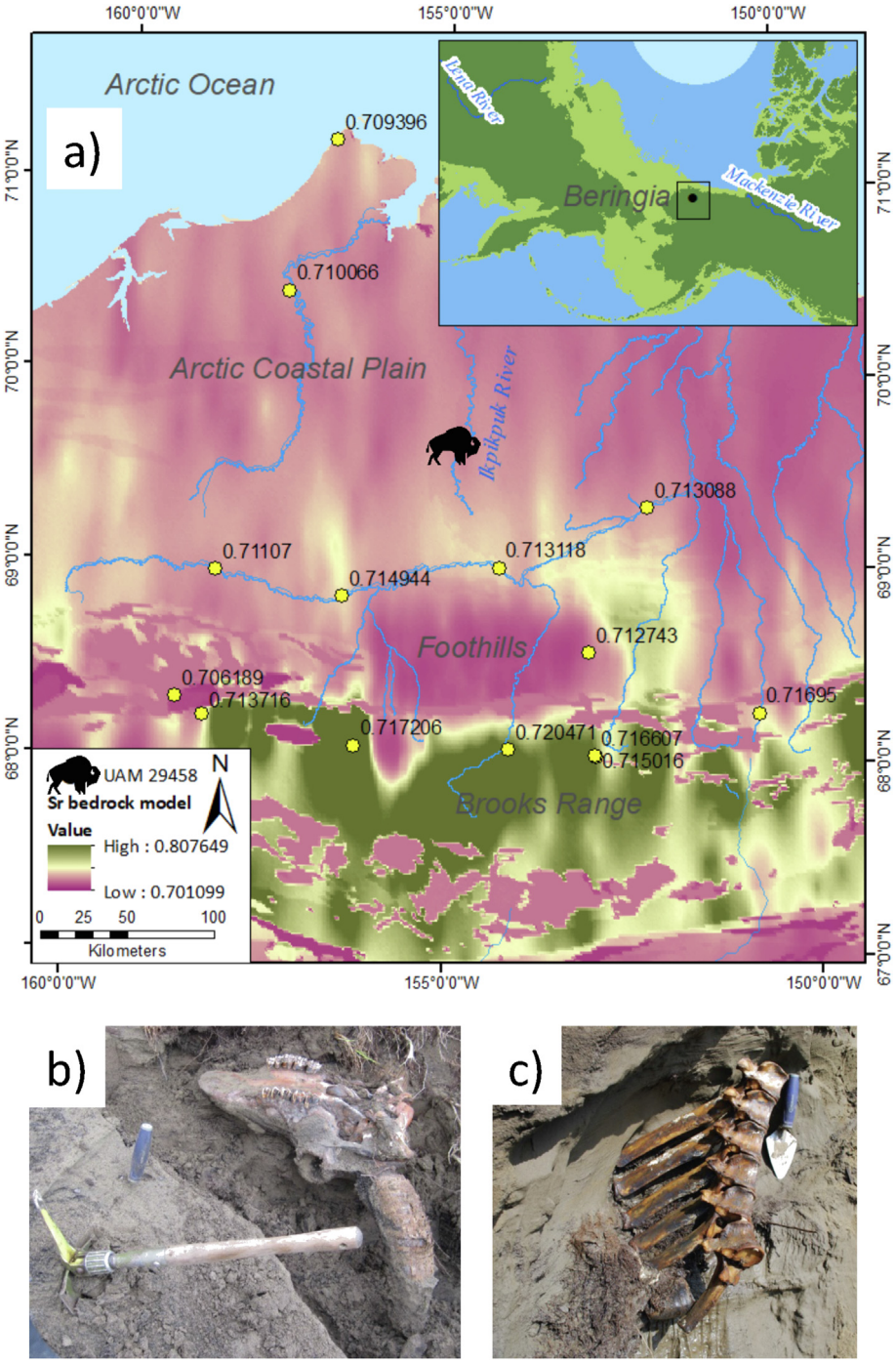

Fig. 1. a) A map on northern Alaska, with the provenance of steppe bison (*Bison priscus*) specimen UAMES 29458 indicated by the black bison icon. Yellow dots show rodent specimen localities and strontium values measured from their teeth. The underlying map is modified from Bataille et al. (2016). b) UAMES 29458 skull in situ during excavation. c) UAMES 29458 articulated thoracic vertebrae attached with connective tissue, in situ during excavation.

2006; Scherler et al., 2014). Examining bison mobility has been one of the more common applications of this isotopic methodology, partly due to the abundance of bison remains in the archaeological and paleontological records (Britton et al., 2012; Julien et al., 2012; Widga et al., 2010).

Stable carbon and nitrogen isotope ratios (expressed as $\delta^{13}C$ and $\delta^{15}N$ values, respectively) from analyses of sub-fossils of animals can add a dietary dimension to a paleoecological reconstruction (Drucker et al., 2008; Stevens and Hedges, 2004). $\delta^{13}C$, along with $\delta^{18}O$, values can be generated from the analysis of inorganic carbon in bones and teeth (Koch et al., 1997). Bison horns, which grow throughout the life of a bison, are a carbon and nitrogen-rich keratin tissue that allows intra- and inter-annual paleoecological inferences. $\delta^{13}C$ values can also be generated from analyses of organic carbon preserved as bone collagen and the horn keratin, and these methods also produce $\delta^{15}N$ values (Iacumin et al., 2001; Schoeninger and DeNiro, 1984). In order to interpret the $\delta^{13}C$ and $\delta^{15}N$ values of these analyses, potential sources of variability need to be evaluated. One common source of $\delta^{13}C$ variation in the diet of herbivores is variation in the proportional contribution C_4 vs. C_3

plants. However, C_4 plants are exceedingly rare or non-existent in the Arctic (Wooller et al., 2007). Furthermore, a lack of trees and even shrubs in Pleistocene Arctic Alaska, even during some warmer interglacials (Willerslev et al., 2014), also excludes "the canopy effect" caused by the concentration of CO_2 in dense forest (Drucker et al., 2008) and differences between herbs and shrubs (Schwartz-Narbonne et al., 2019). Thus, the main source of variability in $\delta^{13}C$ values we can expect in Arctic vegetation is between wetter and drier environments (Wooller et al., 2007).

There are several drivers of $\delta^{15}N$ variation in animals, which can make it a challenging system to study although it often demonstrates important relationships. For example, $\delta^{15}N$ values in ancient megafauna have been found to have a strong relationship with the amount of precipitation during the Pleistocene (Carlson et al., 2016; Drucker et al., 2003; Graham et al., 2016; Heaton et al., 1986; Rabanus-Wallace et al., 2017), which is likely due in part to major changes in soil ecology in response to climatic change (Hobbie and Hobbie, 2006; Stevens et al., 2006). However, for higher resolution $\delta^{15}N$ we must consider behavioral and physiological explanations for change found in serially analyzed tissues (Drucker et al., 2010). Behavioral explanations including migration or dispersal could explain some of the differences and $\delta^{15}N$ values found in relation to aridity (Barbosa et al., 2009) and altitude (Männel et al., 2007). In northern regions, studies have found consistent difference in plants based on mycorrhizal relationships with the soil (Kristensen et al., 2011). However, these are not sufficient to account for the seasonal differences or major regional differences that would be required to explain some of the magnitude of variation in $\delta^{15}N$ values we go on to document in this ancient bison and other modern bison in the region (Funck et al., 2020). Alternatively, physiological changes in $\delta^{15}N$ values of animals can occur in animals adapted to extreme conditions. Notably, animals who undergo hibernation (Lee et al., 2012), lack sufficient calories or are fasting (Hobson et al., 1993; Hobson and Clark, 1992; Mekota et al., 2006; Voigt and Matt, 2004) as well as animals managing acute physical stress (Delgiudice et al., 2000; Fuller et al., 2005; Habran et al., 2010; Rode et al., 2016) can exhibit relatively large increases in $\delta^{15}N$ values. The effect of dietary stress on $\delta^{15}N$ values in wood bison was evident in individuals that had undergone nutritional stress during the winter in Northern Alaska (Funck et al., 2020). For this reason, we will focus our interpretation on nutritional stress as the primary factor of intra-tissue $\delta^{15}N$ variation but acknowledge that other behavioral and ecological factors may be involved. From our review of the literature, we have noted that changes in $\delta^{15}N$ values in herbivores from the mammoth steppe over time have largely not included the possibility that some of the variation could be driven by physiological stress and even starvation. To some degree this is likely obscured by the fact that a majority of the previous research has focused on $\delta^{15}N$ values generated from analyses of bone collagen, which provides a more integrated and essentially a life-time measure. Our analyses of hornsheaths are providing a new a more detailed temporal perspective, which could be translated to the huge abundance of archived bison horn sheaths available. Using a combination of isotopic approaches on different sequentially grown tissues can provide a multi-proxy perspective of an individual's life-history and eventually put this in the context of larger herds.

1.3. Ancient DNA

Ancient DNA (aDNA) from ancient bison specimens from Beringia has been used to monitor gene-flow across the BLB and through the ice-free corridor that connected eastern Beringia to the rest of the Americas (Froese et al., 2017; Heintzman et al., 2016). It has also been used to estimate past changes in effective population size (Lorenzen et al., 2011), which has been used to identify the decline of steppe bison since ~37 kya in Beringia (Shapiro et al., 2004). Analyses using aDNA can also add a further perspective on individual steppe bison specimens. They can provide information on an individual's genomic sex and population affinity, and help constrain age estimates for specimens potentially outside the range or towards the limits of radiocarbon dating. For the latter analysis, one such approach uses Bayesian analysis of aDNA sequences from dated specimens that lived at different time periods to calibrate a molecular clock, and then use this calibration to estimate the age of the undatable individual (Shapiro et al., 2011). The mitochondrial genealogy of Pleistocene bison in North America has been relatively well sampled, both geographically and temporally (Froese et al., 2017; Heintzman et al., 2016; Shapiro et al., 2004), and is therefore likely to be well suited for estimating the age of ancient bison specimens.

2. Material and methods

2.1. Specimen and study site

Dr. Dan Mann and Dr. Pamela Grooves found a nearly complete, and partially articulated specimen of steppe bison (*Bison priscus*) eroding out of a bank of the Ikpikpuk River on the North Slope of Alaska (Fig. 1 a-c) located at 69.71563 N, −154.863 W (WGS 84) (Fig. 1). They excavated and transported it to the University of Alaska Museum (UAM), where the University of Alaska Museum Earth Sciences Collection (UAMES) assigned the catalog number UAMES 29458. The North Slope of Alaska is delimited by the Brooks Range to the south and the Arctic Ocean to the north (Fig. 1). The southern portion is predominantly low foothills that become a coastal plain at ~69° north. The Ikpikpuk River cuts through Quaternary-aged aeolian sand deposits, known as the Ikpikpuk Sand Sea (Carter, 1981). These deposits preserve an abundance of Quaternary vertebrate fossils that erode from banks of the Ikpikpuk River, though rarely in such excellent and complete condition (Mann et al., 2015). The general geology of this region consists of undifferentiated alluvial and aeolian deposits (organic-rich silt, loess and sand) of Holocene to Pleistocene age. The specimen was discovered and excavated from the eroding banks of the Ikpikpuk River in these unconsolidated sediments. The vast majority of vertebrate remains recovered from here are single isolated elements found in reworked sediments while floating the river by small boat. Unfortunately, a quarry map is not available from the site at the time of collection, in part due to the unexpected nature of the find and constraints of rapidly conducting fieldwork in remote Alaska. The sediment and associated microfossils analyzed in this study were collected from matrix directly surrounding or within cavities of the skeleton.

2.2. Fossil material

Skeletal elements of UAMES 29458 were removed from the encasing sediment, cleaned, and anatomically re-articulated (Fig. 2a). Hair, preserved soft tissue, and associated sediment were stored by individual body element and kept frozen. We rearticulated the specimen at the UAMES (Fig. 2 a, b) and examined it for signs of scavenging and other taphonomic processes, using methods outlined elsewhere (Binford, 1981; Domínguez-Rodrigo, 1999; Fisher, 1995; Haynes, 1980; Hudson, 1993; Lyman, 1994, 1987). We found a large number of invertebrate and plant macrofossils within the interstices of the skull, particularly the brain cavity. These were collected and identified to provide taphonomic and paleoenvironmental context. We removed larger macrofossils

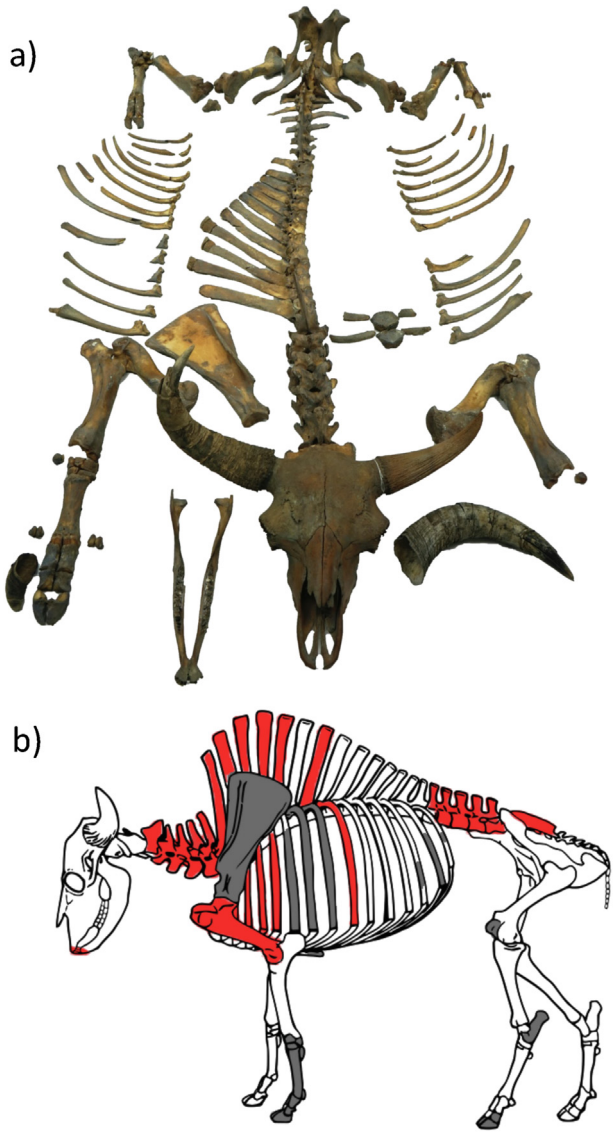

Fig. 2. a) UAMES 29458 rearticulated for taphonomic analysis. b) Skeletal elements missing from specimen are indicated in gray and elements with carnivore marks indicated in red. All elements from the right side were present.

and examined them using a dissecting microscope. We wet sieved sediments at 150 μm and 250 μm. All diagnostic plant macrofossils were collected from sediments larger than 250 μm and all invertebrate materials were collected and archived.

2.3. Radiocarbon analysis

Radiocarbon dating was conducted on different materials associated with UAMES 29458. Previously the bone collagen from the cap of a spinous process, extracted without ultrafiltration, was analyzed at Beta Analytic (Miami, Florida), and found to be non-finite in age >43,500 radiocarbon years (Mann et al., 2013). However, collagen is porous and can be subject to contamination, so we selected additional materials for further analysis, including keratin from the horn sheath, along with a fly pupal case and a plant macrofossil (herbaceous stem) recovered from inside the bison skull. W. M. Keck Carbon Cycle Accelerator Mass Spectrometry Laboratory analyzed the samples on a National Electrostatics Corporation (NEC 0.5 MV 1.5SDH-2) AMS system. The horn sheath keratin was run alongside three non-finite-^{14}C aged bison horn sheath samples and the mean blank from these three was subtracted from sample results, with an assumed 30% uncertainty. All of the sample preparation backgrounds were also subtracted, based on measurements of a^{14}C-free wood standard, with an assumed 30% uncertainty.

2.4. Isotopic analyses

We removed thirty-three intra-tooth subsamples of enamel from the right mandibular molars 1, 2, and 3 (M1, M2, M3) of UAMES 29458 (Supplemental Figure 1). We collected samples in a laminar flow hood at the Alaska Stable Isotope Facility (ASIF) at the University of Alaska Fairbanks (UAF). We removed the surface layer of the target region from each molar and subsequently used a Dremel diamond-coated circular saw to divide samples along each tooth parallel to the growth plane (Figure S1). Enamel samples were removed as chips, which has been found to reduce the potential for contamination (Diego Fernendez, University of Utah, ICPMS Facility, 2018 personal communication).

The University of Utah, Department of Geology and Geophysics, ICPMS facility analyzed half of each sample for ^{87}Sr/^{86}Sr ratios using a multi-collector inductively coupled plasma mass spectrometer (MC-ICPMS - ThermoFisher Scientific, High Resolution NEPTUNE, Bremen, Germany). Strontium isotope analyses followed previously published protocols (Glassburn et al., 2018; Nelson et al., 2018). Additionally, we sampled whole molars from 14 modern rodent museum specimens (I\ UAM Mammalogy Collection; *Microtus oeconomus*, *Microtus mirus, Dicrostonyx groenlandicus*) from within a 250-km radius surrounding the UAMES 29458 locality (Fig. 1a) to determine the bioavailable ^{87}Sr/^{86}Sr ratios in the region (Bataille et al., 2020). This method has previously been used to determine local bioavailable ^{87}Sr/^{86}Sr ratios for comparison to mobile individuals (Hoppe et al., 1999; Kootker et al., 2016; Radloff et al., 2010). The results of this investigation augment existing spatial models of variability in ^{87}Sr/^{86}Sr ratios in Alaska (Bataille et al., 2014).

We chemically pre-treated the remaining half of each bison enamel sample to remove contaminants from gas exchange using the modified method from Pellegrini and Snoeck (2016, 2015) in order to produce δ^{18}O and δ^{13}C values. To compensate for the use of small (~1 × 2 mm) enamel chips rather than powder we increased the soaking time. We added 1 mL of 2% sodium hypochlorite (NaOCl) to each sample, shake to mix, and soaked for 48 h to remove organic particulates. We then rinsed samples with deionized water and soaked them in 1 M acetate buffered acetic acid (0.1 M) (CH_3CO_2H) for 48 h to remove the carbonate portion. Finally, we rinsed the samples three times with deionized water before freezing and then freeze-dried them for approximately 10 h on a VirTiS benchtop Lyo-Centre lyophilizer to remove any moisture prior to isotopic analysis. We analyzed the carbonate fraction using a Thermo Scientific GasBench II carbonate analyzer attached to a Thermo Scientific DeltaV^{Plus} Isotope Ratio Mass Spectrometer at ASIF following previously published protocols (Glassburn et al., 2018). Stable carbon and oxygen isotope ratios are reported in δ notation as parts per thousand (‰) relative to the international standard Vienna Pee Dee Belemnite (VPDB). We ran the samples with laboratory standards of calcium carbonate (Merck, Suprapur 99.95% Lot #B510959 313) every 10 samples to determine analytical precision for δ^{13}C values (0.3‰) and δ^{18}O values (0.2‰) (all errors are expressed as one standard deviations). The δ^{18}O and δ^{13}C values were initially determined relative to VPDB for oxygen and carbon, but the δ^{18}O values were subsequently converted to the Vienna Standard Mean Ocean Water (VSMOW) scale to allow comparison

of the values to meteoric water values. The $\delta^{18}O$ values were converted to VSMOW using Formula 1 (below) (Verkouteren and Klinedinst, 2004) and then Formula 2 (below), a conversion developed by Hoppe et al. (2006) and Velivetskaya et al. (2016) to compare bison enamel to meteoric water $\delta^{18}O$ values:

Formula 1: VSMOW = 30.92 + 1.03092*VPDB.

Formula 2: Enamel carbonate = 0.7(±0.12)*VSMOW-30.06(±1.40).

We removed horn sheath keratin as a wedge perpendicular to the direction of the keratin growth layers (Figure S2). We selected the location to maximize the years of horn growth covered by the core. We then subsampled the core by peeling off thin layers between 0.1 and 0.3 mm in thickness with a razor blade, for a total of n = 113 sub-samples. Sub-samples were analyzed to produce $\delta^{15}N$ and $\delta^{13}C$ values (vs. AIR for nitrogen and VPDB for carbon) using a Flash 2000 Organic Elemental Analyzer (EA) connected via a Conflo IV to an IRMS (DeltaV Plus) at ASIF. Internal reference checks using peptone (No. P-7750 meat-based protein. Sigma Chemical Company, Lot #76f-0300) were run every 10th sample, and blanks were run every 20th sample. Repeated measurements of standards provided the analytical precisions, which were ±0.1‰ and ±0.6‰ for $\delta^{15}N$ and $\delta^{13}C$ values, respectively.

2.5. aDNA analyses

The first premolar (PM1) of UAMES 29458 was sent to the specialized Paleogenomics Laboratory at the University of California Santa Cruz (UCSC) for aDNA analysis. We followed standard protocols as outlined in Froese et al. (2017) to extract and analyze ancient DNA unless stated otherwise. Briefly, we extracted aDNA using a silica column method (Dabney et al., 2013), and then converted extracts into an Illumina-compatible double-stranded DNA library (Meyer and Kircher, 2010). We enriched an aliquot of this DNA library for bison mitochondrial genomic fragments using a commercial MyBaits target capture kit (Arbor Biosciences, Ann Arbor, MI). We sequenced both the enriched and remaining unenriched library on separate runs of an Illumina MiSeq using v3 150 cycle chemistry75 cyc, with paired-end 75 bp reads. We then merged the paired-end read data, trimmed adapters, and removed short (<25 base pairs (bp) for the enriched library; <30 bp for the unenriched library) and low-complexity sequences (DUST cutoff: 7) using SeqPrep and PRINSEQ-lite v0.20.4 (Schmieder and Edwards, 2011).

We aligned the filtered reads from the unenriched library to a reference database that included the cow (*Bos taurus*) genome (Genbank: Btau_4.6.1) and an American bison (*Bison bison*) mitochondrial genome (Genbank: NC_012346), using the Burrows Wheeler Aligner (BWA; Li and Durbin, 2009) aln algorithm with the seed disabled (-l 1024). We filtered aligned reads by map quality score (minimum of 20) and removed duplicates using SAMtools v0.1.19 (Li and Durbin, 2009). We assessed aDNA damage patterns using mapDamage v2.0.9 (Jónsson et al., 2013). To infer the genomic sex of UAMES 29458, we followed the method of Heintzman et al. (2017), which compares the relative mapping frequency of the X chromosome to the autosomes. A male is inferred if this ratio is 0.45–0.55, whereas the expectation for a female is 0.95–1.05.

We mapped the filtered reads from the enriched library to a steppe bison reference mitochondrial genome (Genbank: KX269138) using the multiple iterative assembler (MIA; Briggs et al., 2009) and BWA, as above. For aDNA damage assessment of the enriched data, we used the BWA mapping consensus results as the reference sequence for mapDamage. We calculated a mitochondrial genome consensus sequence from the MIA mapping results using the criteria outlined in Froese et al. (2017), and added this sequence to the full mitochondrial genome alignment of Froese et al. (2017), as modified by Zazula et al. (2017). This alignment consisted of four yak and 47 Siberian or North American bison mitochondrial sequences.

Before estimating the age of UAMES 29458 with Bayesian time-tree methods, we tested for temporal signal in the data set. Tip-dating methods are only valid if this signal is present, as these methods will usually converge on an estimate whether or not there is a temporal signal present (Firth et al., 2010). We used a linear regression of phylogenetic root-to-tip distance against the sampling date to test for temporal signal (following Murray et al., 2016). We estimated a neighbor-joining tree of the data set (excluding the yak and two radiocarbon non-finite bison sequences) using a K80 nucleotide substitution model with pairwise deletion, using the ape package in R (Paradis et al., 2004), in which the root was fit simultaneously with the regression, so as to minimize the residual mean squares, with the resulting root matching the root obtained by using the yak sequences as an outgroup. Analyses of the full alignment and a reduced alignment, with MS022 omitted (see below), returned positive correlations that are significantly different from random permutations over clusters of samples with similar dates (full: $r = 0.50$, $p = 0.010$; reduced: $r = 0.44$, $p = 0.025$; Figure S3). We defined similar-date clusters (n = 34–35) as monophyletic clades that had the same date after rounding to the nearest thousand years. A Mantel test suggested that this clustering was sufficient to eliminate a correlation between genetic and temporal distances in the data (without clustering: $p = 0.001$, with clustering: $p = 0.18$) (Murray et al., 2016), which can result in a false positive result. Overall, these analyses suggest the presence of temporal signal in the bison mitochondrial genome data set.

We then estimated a time-tree in BEAST (v1.10.4, Drummond et al., 2012) so as to estimate both the age of UAMES 29458 and its placement in the bison mitochondrial genome phylogeny. We used a strict molecular clock with either finite radiocarbon dates or stratigraphic data associated with the other sequences in the analysis as priors, following Froese et al. (2017) and Zazula et al. (2017). To estimate the age of UAMES 29458, we used a uniform prior distribution of between 30 kya BP (as this specimen is borderline radiocarbon finite; see results) and 195 kya BP (the earliest mitochondrial estimate for the arrival of bison in North America; Froese et al., 2017), following the method of Shapiro et al. (2011). To test the robustness of the oldest age estimates, we also ran analyses with the minimum age prior set at 0, 20, 40, or 50 kya BP. We ran analyses with each set of priors twice, each time with the Markov chain Monte Carlo (MCMC) chains run for 60 million iterations, sampling every 3000 iterations, and discarding the first 10% as burn-in. Using Tracer v1.6, we observed that all parameters reached convergence with the exception of the tree likelihood, which swapped between two optima in all analyses. This was due to the shifting placement of sequence MS022 (KX269130; Froese et al., 2017). This sequence was therefore removed from the alignment and all analyses were re-run. Convergence was then observed for all parameters. For each prior and alignment result set, we summarized trees and calculated a maximum clade credibility tree. All ages are reported as 95% highest posterior density (HPD) credibility intervals.

3. Results

3.1. Physical description

Overall, we observed UAMES 29458 to be relatively complete and well preserved (Fig. 2). Based on the observed number of annual growth cycles visible in the horn sheath, we estimated the bison specimen to be minimally 12 years old, which is considered a

mature individual (Fuller, 1959). The specimen's horn span was 90 cm at the widest point and the comparative angle and length of the horns indicate that it was a male (Guthrie, 1966). Much of the hair had sloughed off the specimen and was found in the surrounding sediment. In some areas, hair and skin had dried to the bone and were still attached. Hair from the front and hind limbs was yellow ochre in color, as were the shorter undercoat hairs from the body. The longer hairs were a reddish-brown or dark brown and tail hairs were black to dark brown. Long hairs found in the surrounding sediment, which likely came from the cape (hair on the shoulders), beard (long hair on the chin) or cap (long hair on the top of the head), were light to dark brown.

The skull was in excellent condition and the left and right mandibles were fused at the symphysis. The incisors were missing from a pre-burial break. There were no gnaw marks on the surrounding bone to indicate another animal had gnawed them off. Evidence of root etching was observed on the ventral surfaces of the mandible with vivianite deposits observed on the articular surface. Vivianite was identified visually, it is commonly found on fossils found in these environments, and is unique in its blue appearance. We observed that the cervical vertebra 2 (C2) through thoracic vertebra 7 (T7) had the dorsal portion of the spinous process gnawed (Fig. 3b) and bitten off (Fig. 3a). We also observed T4 and T5 had evidence of damage from a carnivore, including puncture marks (Fig. 3 a). Lumbar vertebra 1 (L1) to the sacrum also had evidence of carnivore damage on the ventral surface of the vertebrae (Fig. 3 b). The distal ends of four thoracic ribs (towards the anterior portion of the body) also had puncture marks and gnawing. There were several pre- and post-burial breaks, and several medial portions of the ribs were missing. One rib on the right side had a pathology consistent with a healed break (Fig. 3c). Two thoracic ribs were missing from the left side. The costal cartilage had carnivore gnawing damage on two fragments and the manubrium was missing one section.

The right appendicular skeleton was complete and we observed no evidence of carnivore damage. In addition, there was soft tissue (keratinous hoof sheathes, leather-like flesh and connective tissue) and vivianite present. There were gnaw and puncture marks observed on the proximal end of the left humerus (lateral tuberosity) near its articulation with the scapula; the scapula was missing. There was root etching on the medial surface of the humerus where it would have rested on the ground after the specimen's death and we observed soft tissue adhering to the bone. The left metacarpal, carpals, and proximal, medial, and distal phalanges were missing, which could be consistent with loss during taphonomic processes upon emerging from the riverbank because the bones would have been exposed first and eroded out of the bank. In addition to the lack of carnivore marks near the articulations, they do not possess much food value for a carnivore and would not have been a primary target. On the left femur there was a pre-burial break at the greater trochanter, but no obvious carnivore damage. The left patella, calcaneus, several left tarsals, one sesamoid, one proximal, medial and distal phalanx was missing, which is also consistent with secondary loss upon the specimen eroding out of the riverbank.

3.2. Radiocarbon analysis

We generated three new radiocarbon dates associated with UAMES 29458 (Table 1). The background-subtracted fraction modern values for both the keratin and insect chitin are different from zero by ~6 standard deviations, which indicates the ages are finite. The age of the keratin from the bison horn sheath was 46,000 ± 1100 ^{14}C yr BP (46,962 cal yr BP using CALIB 7.1 (Stuiver et al., 2019)), which was very similar to the radiocarbon date produced from the keratinous fly puparium (Table 1, Fig. 4) taken from inside the bison skull cavity (46,800 ± 1200 ^{4}C yr BP, just outside

Table 1
Summary of radiocarbon dates.

Material	^{14}C yrs	Error	Cal yr BP CALIB	Laboratory	Accession Number
Collagen	>43,500	NA		BETA	324600
Keratin	46,000	1100	46,962	Keck	209861
Chitin	46,800	1200		Keck	209862
Plant	>49,990	NA		Keck	209863

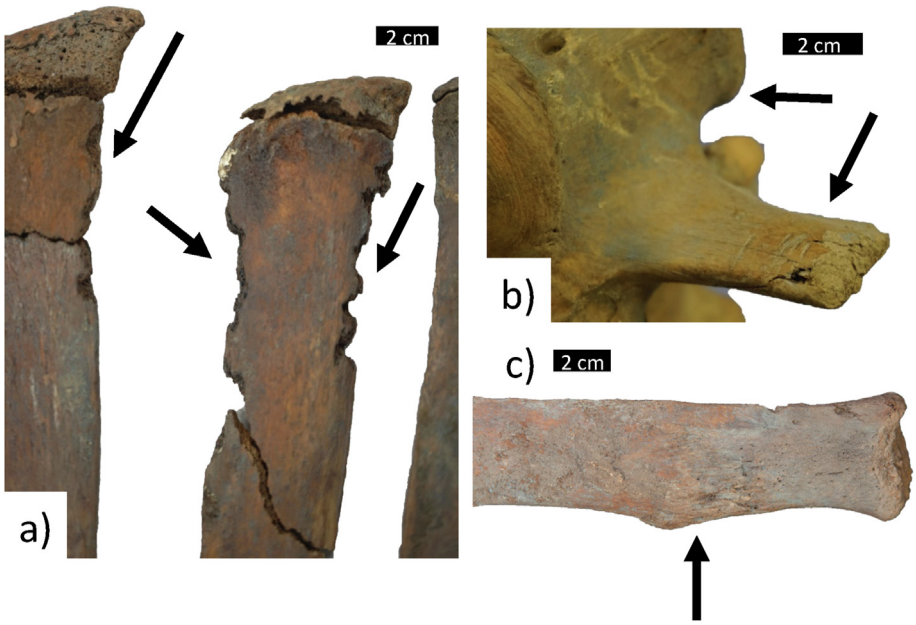

Fig. 3. Scavenger dentition marks on the a) thoracic spinous processes of *Bison priscus*, UAMES 29458 with bites indicated by arrows, and b) ventral side of lumbar vertebrae with gnaw marks indicated by arrow. c) Rib with healed pathology indicated by arrow.

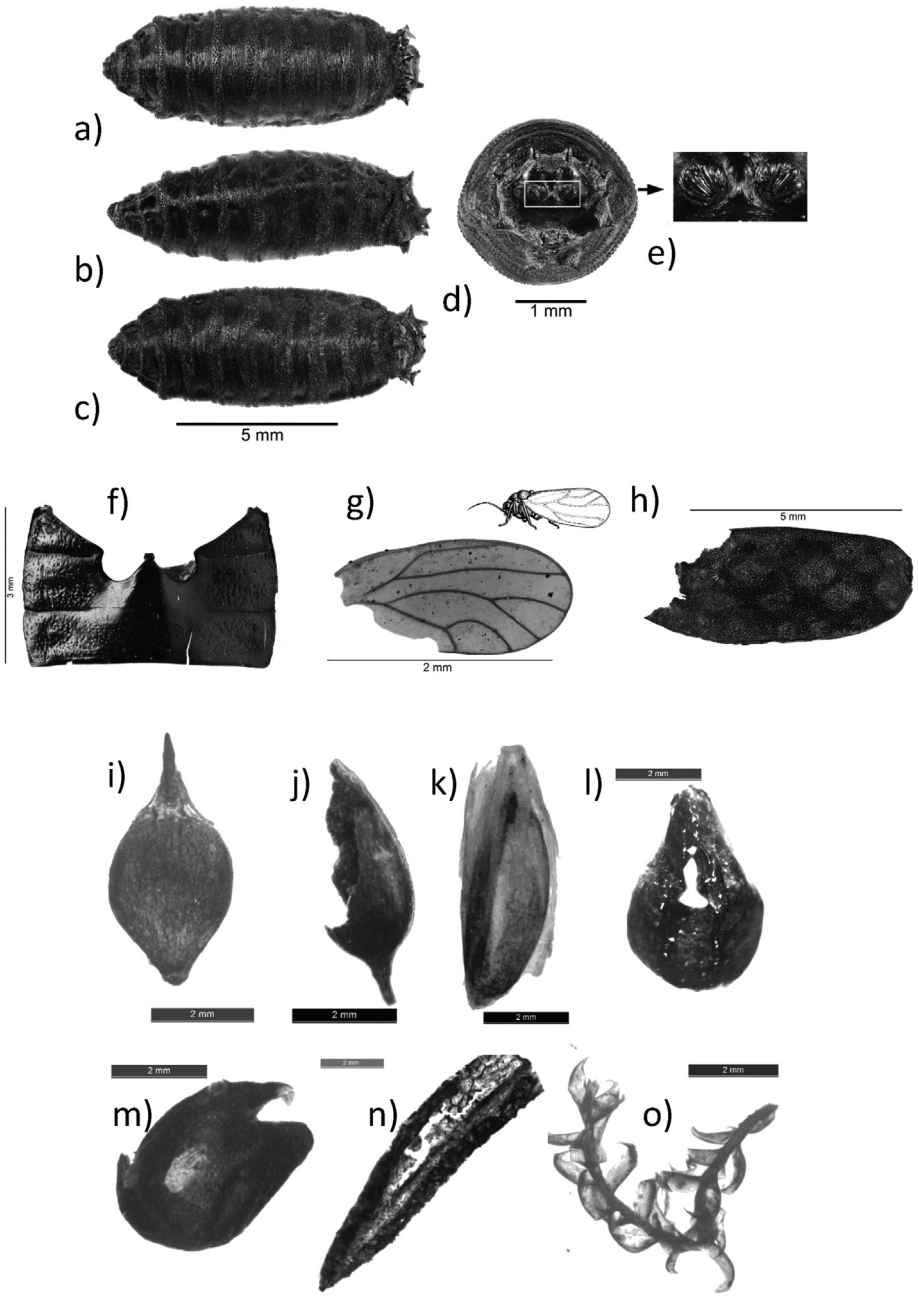

Fig. 4. The macrofossil assemblage taken from the skull of UAMES 29458: *Protophormia terraenovae* puparium UAMES 52319. a), dorsal view b), lateral view c), ventral view d), posterior view, the posterior spiracles surrounded by a rectangle e), the posterior spiracles in close-up view. (photos: J.-B. Huchet, 2018), f) Partial abdomen sternites of a ground beetle UAMES 52334 (Carabidae: Pterostichinae) (photo: J.-B. Huchet, 2018), g) Psyllid forewing recovered from inside the bison skull UAMES 52331 (photo: J.-B. Huchet, 2018), h) Right elytron of a ripicolous ground beetle of the genus *Elaphrus* Fabricius UAMES 52333 (Carabidae: Elaphrinae) (photo: J.-B. Huchet, 2018), i) *Carex* seed lenticular, j) *Carex* seed trigonal, k) Poaceae caryopsis, l) *Polygonum bistorta*, m) *Draba*-type seed, n) *Andromeda polifolia,* o) *Bryophyta* sp.

the range for calibration using CALIB 7.1 (Stuiver et al., 2019). The dated plant macrofossil found in the skull, along with the puparia, had a radiocarbon date of >49,900 radiocarbon years, which was outside the range for calibration (Table 1).

3.3. Macrofossils

3.3.1. Fossil plant remains

The contents of the neural canal of the spine and skull from UAMES 29458 included a sand-rich matrix with abundant moss, wood, and we could identify other plant fragments to species in some instances (Figs. 4 and 5). The plant macrofossil assemblage from inside the skull is consistent with a mesic tundra or a wet flood plain surrounded by a shrub tundra (Fig. 5). The presence of *Daphnia* spp. ephippia indicate that the sediment was also, at least partially, aquatic in origin. Bryophytic material, likely from wet tundra and rivers, was abundant and well preserved in the skull cavity. Wood was very common and possibly came from the shrubs identified from seeds, leaves, and other materials in the skull cavity, including *Salix* spp. (willow), *Betula* spp. (birch), and *Andromeda polifolia* (bog rosemary) (Fig. 4 n). These shrubs are typical of wet tundra and tend to be more abundant in more protected areas

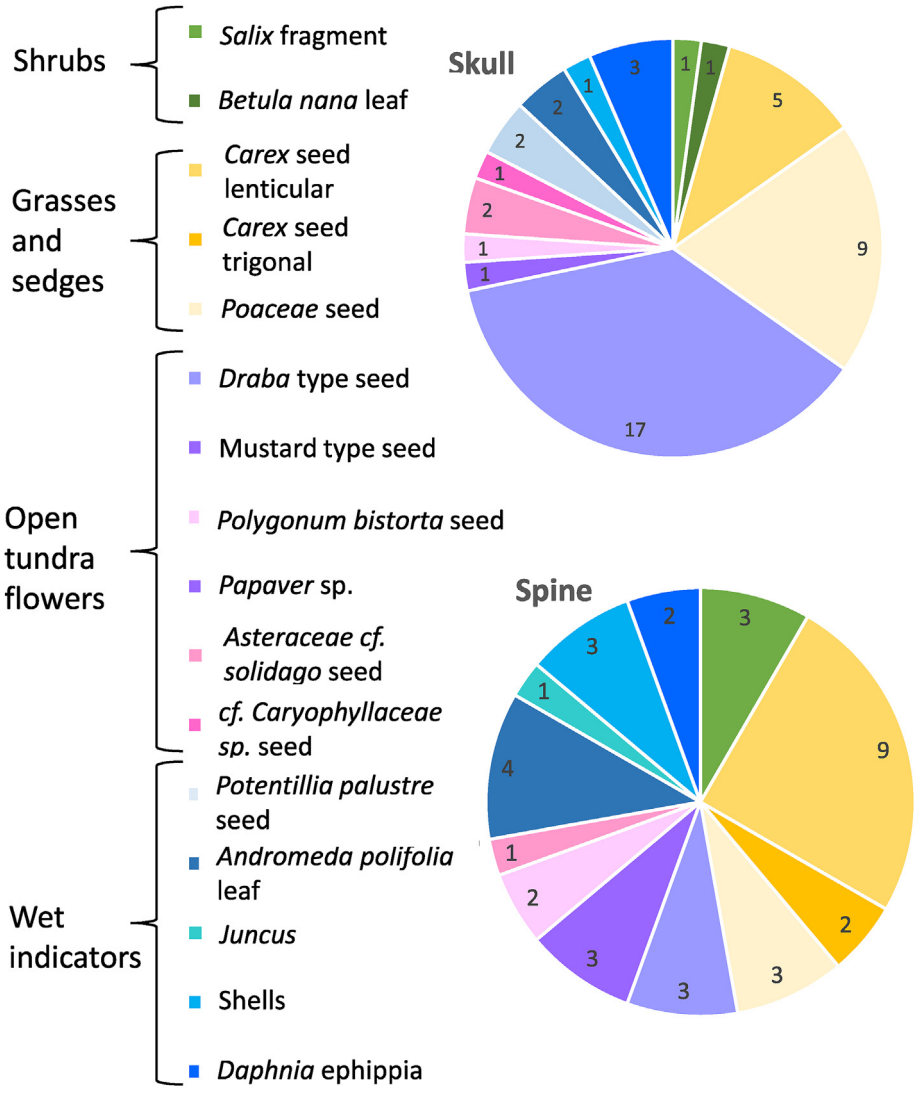

Fig. 5. The relative abundance of plant macrofossil specimens in the skull and spine of UAMES 29458, categorized by characteristic eco-type.

(Cody, 2000; Hulten, 1968), suggesting an interstadial environment. In addition, *Potentilla palustris* and *Juncus* spp. were also present and are typically associated with riparian habitats and bogs (Cody, 2000). In contrast, the remains of *Papaver* spp. (poppies) and *Polygonum bistorta* (Fig. 4 l), which favor drier open slopes (Hulten, 1968), were also present in the bison skull cavity. The largest number of plant macrofossils from the skull cavity was the mustard and *Draba*-type seeds (Figs. 4 m and 5), which are from a large and very diverse family making it difficult to use these specimens to characterize paleoecological conditions (Cody, 2000; Hulten, 1968). However, many of the species from this group are typical of open slopes, gravel and/or sandy river banks (Cody, 2000). In addition, there is a portion of grasses (Poaceae) (Fig. 4 k) (and *Carex* Fig. 4 i and j) that are typical of tundra or steppe ecosystems in the Arctic, and are consistent with an open landscape with no large shrubs (Hulten, 1968). The burial occurred in a time scale that prevented extensive skeletal disarticulation by scavengers but allowed some activities by insects in an energy regime that allowed deposition of sand but not coarser sediment.

3.3.2. Fossil insect remains

Analysis of the skull cavity of UAMES 29458 revealed the presence of insect remains, including complete or incomplete blowfly puparia (Calliphoridae) (n = 15, UAMES 52319–52330). From their excellent state of preservation, a determination at the species level was possible and the taxon that colonized the bison at the time of its death was identified as the northern blowfly *Protophormia terraenovae* (Robineau-Desvoidy) (Fig. 4 a-e). With the exception of 4 fragmentary specimens, all the puparia were complete and unhatched indicating that the life cycle was interrupted before adult emergence. An attempt to open two fossil puparia, in order to find a possible nymph and to observe its maturity stage, proved unsuccessful since the pupa had disintegrated inside.

Partial abdomen remains of a carabid beetle (Pterostichinae: cf. *Pterostichus* sp.) were also found inside the skull (UAMES 52334; Fig. 4 f). Thirty-five *Pterostichus* species occur in Alaska (Bousquet et al., 2013). Some representatives of this genus (i.e. *Pterostichus costatus* Ménétriés), live in the damp peaty areas of lowland tundra regions (Lindroth, 1966). Other insect remains belonging to several

distinct orders were also recovered from inside the skull: a complete wing of Psylloidea (Homoptera) (UAMES 52331; Fig. 4 g); a cephalic capsule of a larval Chironomidae (Diptera), an incomplete elytron of Elaphrinae (Coleoptera, Carabidae) (UAMES 52332; Fig. 4 h) and finally, some disarticulated coleopteran remains, too fragmented to be identified. The presence of a psylloidean species in this context is not surprising since fossil remains of the three main plants (*Salix, Betula, Polygonum*) exploited by these insects were preserved evidenced within the skull cavity of the bison. The larval stages of chironomids develop in almost any aquatic or semiaquatic habitat, both standing and flowing waters, but also occur in tree-holes, rotting vegetation, and damp soils. Finally, the presence of *Elaphrus* sp. (cf. *trossulus* Semenov) (UAMES 52333; Fig. 4 h), another ground beetle, is recorded. The species belonging to this genus are representative of riparian communities. Adults of all species of *Elaphrus* live along rivers, small streams, swamps, sloughs, or bogs, which is fully consistent with the bison discovery site. Overall, these taxa are typical of mesic to wet tundra habitats at the time of burial.

3.4. Isotopic analyses

The $\delta^{13}C$ and $\delta^{15}N$ values from the collagen sample were −20.0‰ (±0.6) and 4.2‰ (±0.1), respectively. The $\delta^{13}C$ value is consistent with a diet of vegetation consists of plants using C_3 photosynthesis in a relatively open environment (Drucker et al., 2008). The $\delta^{15}N$ value is consistent with values from other bison specimens dated to interstadial conditions, and contrast with stadial conditions, which can have higher values (Hedges et al., 2004; Rabanus-Wallace et al., 2017). Based on an 8−10 year collagen turnover rate (Hedges et al., 2007), the collagen would exclude the higher $\delta^{15}N$ values from this individual's early life based on analyses of the horn sheath (described below), and thus the bone collagen and horn can be considered in the same range. The mean horn keratin $\delta^{13}C$ value was slightly lower than the collagen values (mean $\delta^{13}C$ value −21.3‰ ±1.1; −20.0‰ respectively), which is consistent with the difference in fractionation factors associated with the two different tissue types (keratin $\Delta = 3.1‰ \pm 0.3$; collagen $\Delta = 5.1‰ \pm 0.3$ (Drucker et al., 2008)).

The mean $\delta^{15}N$ value from analyses of the horn keratin (4.6‰ ±1.1) was similar to the $\delta^{15}N$ value from the collagen value (4.2‰ ±0.1). The periodicity of the isotopic fluctuations in the horn sheath (Fig. 6) appears to reflect annual cycles because the number of oscillations (n = 11) is consistent with the number of observed annual growth layers observed from the horn (11−12). The first two oscillations (~2 years) likely correspond with the period covered by the tooth record (~2.5 years) from the same specimen (described below). These apparently annual fluctuations would be consistent with the peaks in $\delta^{15}N$ values reflecting a seasonal shift to greater nutritional stress and a more water-limited plant diet during the winter 2020). Shortly before the death of the bison, the $\delta^{15}N$ values from the horn sheath increases (Fig. 6), which would correspond with a transition from summer to winter that is observed in modern bison from Alaska (Funck et al., 2020), indicating the bison may have died in the late summer/early fall. Two peaks in the $\delta^{15}N$ values from the horn sheath occurred towards the start of the life of the bison and the second of these corresponds with a decrease in $\delta^{13}C$ values from the horn sheath. These features are consistent with periods of nutritional stress (Funck et al., 2020). Most notably, this pattern seems consistent with catabolism and the use of lipid reserves respectively (Funck et al., 2020). A marked decrease in $\delta^{13}C$ values is evident in the year prior to the bison's death, which also seems consistent with the use of the animal's lipid reserves (Funck et al., 2020).

The results of the strontium isotope analyses (n = 33) of UAMES 29458 (Table 2), with an analytical precision of 0.00001, show a mean $^{87}Sr/^{86}Sr$ ratio from the first molar (M1) of 0.71139 (±0.00028). These values are consistent with the rodent teeth values from the Arctic Coastal Plain, which range from 0.70940 to 0.71107 (Table 3, Fig. 7). The mean $^{87}Sr/^{86}Sr$ ratio from the M2 was higher compared to the values from the M1 ($p < 0.000$, t.test), averaging at 0.71206 (±0.00025). The mean $^{87}Sr/^{86}Sr$ ratio from the M3 was 0.71308 (±0.00008) and was higher than the values from both the M1 and M2 ($p < 0.000$, t.test). The range of the M3 values was similar to the values found from the modern rodents found in the foothills of the Brooks Range (Table 3) (from 0.7137 to 0.7205) (Fig. 8). Based on the bedrock $^{87}Sr/^{86}Sr$ model (Bataille and Bowen, 2012), the expected $^{87}Sr/^{86}Sr$ ratio at the place of death of UAMES 29458 was ~0.70982 (Fig. 8). Overall, the M1, M2 and M3 sequential data show a marked increase in $^{87}Sr/^{86}Sr$ ratios throughout the tooth sequence ($p < 0.000$, ANOVA) (Fig. 7).

The mean $\delta^{18}O$ value across all teeth samples from UAMES 29458 (n = 30) was −21.1‰ (±0.4) vs. VPDB (with an analytical precision of 0.2‰) (Table 4). Values were highly variable across the M1-M3 sequence (Fig. 7) ranging from −18.4‰ to −26.5‰, but were not significantly different between teeth ($p = 0.34$, ANOVA). The values appear to cycle through approximately two full years, with three peaks representing summers, which seasonally have higher $\delta^{18}O$ values (Velivetskaya et al., 2016) and separated by two cooler periods with lower values (Fig. 7).

The mean $\delta^{13}C$ value of the enamel calcium carbonate from the teeth of UAMES 29458 was −11.0‰ (±2.0) (with an analytical precision of 0.03) and had a relatively small range of values (−10.3‰ to −11.7‰) (Table 4), which are consistent with a C_3 diet. Typical values for C_3 plants are ~ -27‰ (Wooller et al., 2007) and the difference between animal diets and tooth calcium carbonate is Δ+14.6 - (Cerling and Harris, 1999; Passey et al., 2005). Overall the $\delta^{13}C$ values started at their lowest during early life (M1) and gradually became higher in the M2 (−11.1‰ ±0.2) and M3 (−10.5‰ ±0.1) ($p < 0.000$, ANOVA), a trend that appears to correlate with the temporal shift from lower to higher $^{87}Sr/^{86}Sr$ values from the same teeth (Fig. 7).

3.5. aDNA analyses

We generated 1.15 million reads from the unenriched library of UAMES 29458 (raw reads available at the NCBI Short Read Archive under BioProject PRJNA61324), which had an endogenous DNA content of 15.4% based on reads aligning to the cow genome. The relative mapping frequency ratio between the X chromosome and autosomes was 0.528, with a range of 0.493−0.561 across all 29 autosomes (Table 5). This is consistent with UAMES 29458 representing a genomic male individual.

A full mitochondrial genome (JK319) was generated from the enriched library, with an average coverage of 139 × (Genbank: MN549280). The phylogenetic placement of the UAMES 29458 mitochondrial genome was marginally impacted by the minimum age prior used, and was found either to fall at the base of Clade 2 (prior of 50 kya BP) or to be sister to MS002 within bison mitochondrial Clade 2 (all other tested priors) (Fig. 9, Table 6). The inclusion or exclusion of MS022 did not affect the phylogenetic placement of UAMES 29458. Across all analyses, the age of UAMES 29458 was estimated to be ~33−87 kya BP (Table 6). Analyses with MS022 excluded generally yielded slightly older age estimates, but varying the minimum age prior did not greatly impact this individual's maximum estimated age (range of ~81−87 kya BP across all analyses). This suggests that the priors did not drive the estimated age results.

Mapped reads from both the unenriched (primarily nuclear) and enriched (mitochondrial) DNA libraries exhibit damage patterns

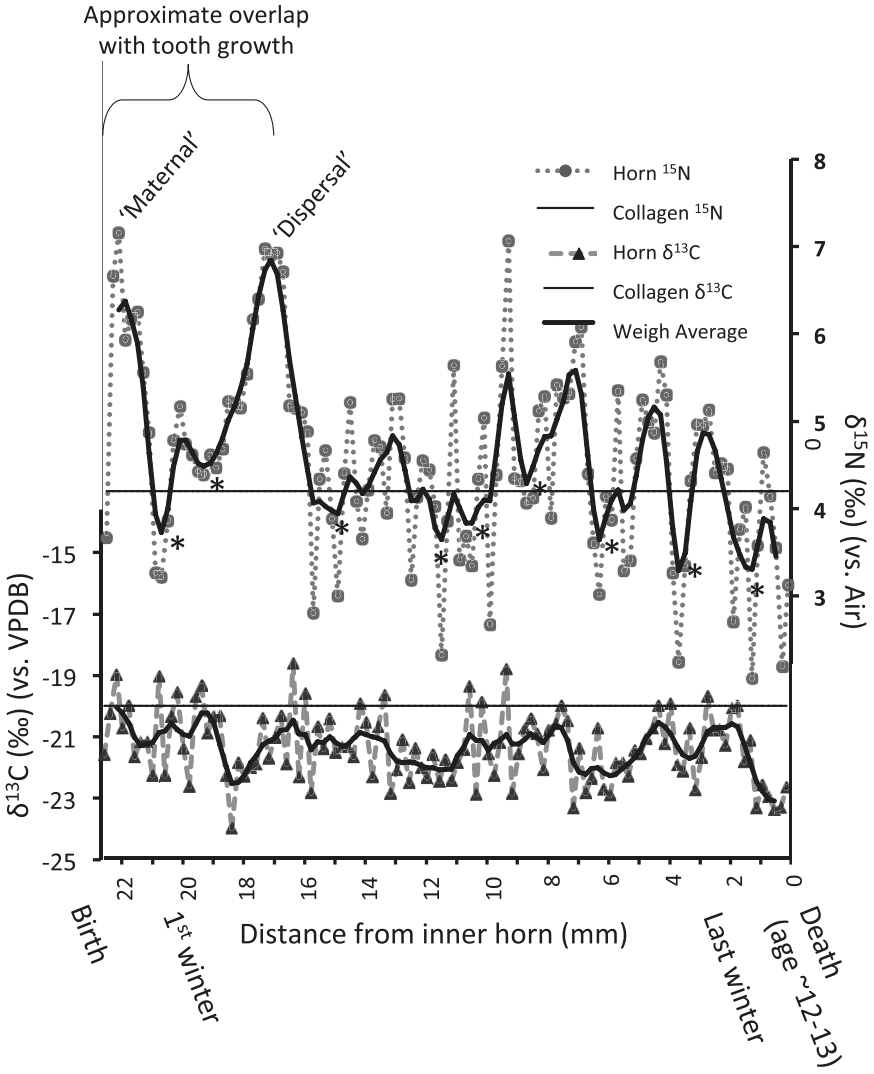

Fig. 6. Carbon and nitrogen stable isotope values of serial horn sheath samples (n = 113) with dotted trend-line of weighted moving averaging of the nearest 3 samples and bulk collagen carbon and nitrogen stable isotope values. * Indicate lowest δ^{15}N values associated with summer. Labels on the bottom indicate approximate timing of identifiable life events.

characteristic of authentic aDNA, including short DNA fragments and elevated relative deamination frequencies at the ends of reads (Figure S4).

4. Discussion

4.1. Constraining a chronological age for UAMES 29458

UAMES 29458 provides several lines of evidence that can be used to constrain the individual's chronological age (Fig. 11). The radiocarbon dates from the keratin and the blow fly puparium (chitin) are nearly identical (46,000 ± 1100 ^{14}C yrs and 46,800 ± 1200 ^{14}C yrs – inside and outside the range for calibration, respectively). Keratin is a structurally dense tissue and less susceptible to contamination than collagen (Taylor et al., 1995). The blow fly *Protophormia terraenovae*, which colonizes a corpse within hours or days following death, seemed a good candidate for precise ^{14}C dating of UAMES 29458. The congruence of the keratin and chitin ^{14}C dates lends support for a finite age of approximately 46,900 ^{14}C yrs. In contrast, the radiocarbon dates from collagen and from plant material are non-finite. Collagen, from porous bone material, can be contaminated or degraded. The sample from the bone of UAMES 29458 was also run on a lower energy ^{14}C instrument, which cannot discriminate low levels of ^{14}C from old samples compared with the chitin and keratin, which were run on a more powerful instrument. The radiocarbon date of the plant material and its apparent older age compared to the puparium and keratin is difficult to interpret. The plant material recovered from the skull was specifically selected because it was a delicate herbaceous structure that would not have substantial reworking or be influenced by variations in carbon sources that can occur in aquatic plants (Marcenko et al., 1989). However, the radiocarbon date of the plant was determined to be non-finite (>49,000) and could have been reworked from older sediments. Given that the dates from keratin and chitin are on the margins of radiocarbon limits we must consider two possibilities; first, that the finite dates are accurate, or second, that these dates are not distinguishable from non-finite dates.

Other evidence supports the hypothesis that UAMES 29458 dates are finite in age. Environmental information from the δ^{18}O

Table 2
Results of isotopic analysis of strontium, carbon and oxygen of UAMES 29458.

Tooth	Sample #	Distance from base of enamel (cm)	$^{87}Sr/^{86}Sr$	$\delta^{13}C$ ‰ (VPDB)	$\delta^{13}C$ ‰ Std dev	$\delta^{18}O$ ‰ (VPDB)	$\delta^{18}O$ ‰ Std dev
M1	1	1.8	0.71117	−11.4	0.1	−19.0	0.1
	2	1.7	0.71087	−11.5	0.3	−20.2	0.3
	3	2.55	0.71116	No data	No data	No data	No data
	4	1.3	0.71132	−11.3	0.4	−21.0	0.5
	5	1.15	0.71125	−11.4	0.5	−23.8	0.9
	6	1	0.71138	−11.0	0.2	−21.0	0.2
	7	0.8	0.71144	−11.2	0.3	−22.1	0.4
	8	0.65	0.71158	−11.3	0.1	−22.2	0.2
	9	0.5	0.71162	−11.2	0.1	−22.2	0.2
	10	0.3	0.71172	−11.7	0.4	−23.2	0.4
	11	0.2	0.71182	−11.4	0.2	−22.1	0.3
M2	1	2.1	0.71172	−10.7	0.1	−18.8	0.3
	2	1.95	0.71184	−10.9	0.2	−19.7	0.6
	3	1.8	0.71198	−11.0	0.1	−19.6	0.1
	4	1.65	0.712	−11.5	0.3	−22.7	0.4
	5	1.45	0.71189	−10.7	0.2	−20.2	0.4
	6	1.35	0.71191	−10.9	0.2	−20.5	0.5
	7	1.1	0.71195	−11.4	0.2	−21.7	0.3
	8	0.95	0.71195	−11.5	0.5	−26.5	0.9
	9	0.75	0.71214	−11.3	0.1	−21.2	0.3
	10	0.6	0.71242	−11.4	0.1	−21.5	0.3
	11	0.45	0.71236	No data	No data	No data	No data
	12	0.3	0.71255	No data	No data	No data	No data
M3	1	2.25	0.71297	−10.9	0.1	−22.3	0.3
	2	2.05	0.71324	−10.5	0.1	−21.0	0.1
	3	1.8	0.71315	−10.5	0.4	−21.0	0.1
	4	1.60	0.71314	−10.9	0.2	−22.3	0.2
	5	1.4	0.71307	−10.5	0.2	−21.1	0.3
	6	1.2	0.71302	−10.3	0.1	−19.7	0.1
	7	1	0.71303	−10.4	0.2	−20.0	0.2
	8	0.85	0.71298	−10.4	0.2	−20.0	0.2
	9	0.6	0.71303	−10.4	0.1	−18.4	0.2
	10	0.45	0.71304	−10.6	0.2	−20.0	0.2

Table 3
Rodents use for characterizing $^{87}Sr/^{86}Sr$ isoscape.

UAM Mamm #	Species	Locality	$^{87}Sr/^{86}Sr$
4650	*Microtus oeconomus*	Meade River village	0.71007
8163	*Microtus oeconomus*	Umiat region, 1 mi N Umiat	0.71309
11149	*Microtus oeconomus*	Kikitaliorak Lake, Noatak drainage, ca 18 mi ESE Howard Pass	0.71721
11166	*Microtus oeconomus*	Feniak Lake (Noatak Valley, Feniak Lake, Makpik Cr)	0.71372
13614	*Microtus oeconomus*	Barrow, NARL research facilities	0.70940
56327	*Microtus oeconomus*	Desperation Lake	0.70619
66866	*Microtus miurus*	Unknown	0.71274
78833	*Microtus miurus*	Agiak Lake	0.71502
79046	*Microtus miurus*	Nanushuk River	0.71695
79102	*Microtus oeconomus*	Agiak Lake	0.71661
82113	*Microtus oeconomus*	N side of Lake Tulilik	0.72047
125703	*Microtus oeconomus*	Colville River - confluence of Kiligwa	0.71107
125706	*Dicrostonyx groenlandicus*	Colville R and confluence of Ipnavik	0.71494
125713	*Microtus oeconomus*	Colville River - SE of Kakvuiyat Bend	0.71312

values from the bison specimen and plant macrofossils add further dimensions that help constrain the chronological age estimation for UAMES 29458. The mean $\delta^{18}O$ value (as VSMOW) from analyses of the bison's molars is −3.9‰ (±1.2) lower than the mean modern precipitation values. In contrast, full stadial $\delta^{18}O$ values for precipitation tend to be around −8% lower than modern precipitation values (Bowen, 2018; Gaglioti et al., 2017; Meyer et al., 2010; Rasmussen et al., 2014). The $\delta^{18}O$ values from UAMES 29458 therefore indicate that although the climate was slightly colder than modern it was not full stadial (Fig. 11). The finite radiocarbon date from the keratin coincides with a period of time that had an offset in $\delta^{18}O$ values of Δ −3.9‰ (±1.2), between 44,380 cal yrs BP and 46,880 cal yrs BP (Rasmussen et al., 2014). This inference that the bison specimen may have lived during a more moderate (interstadial) climate is also supported by the plant macrofossils and insect remains found in the skull, which represent a typical flood plain in tundra ecosystems of the Arctic. However, as stated above, the plant remains may not be exactly contemporaneous with the specimen.

The Bayesian molecular age estimate for the specimen was between ~33 and 87 kya BP, which is consistent with the radiocarbon ages and corresponds to Marine Isotope Stage (MIS) 3 through to MIS 5 b (Lisiecki and Raymo, 2005). Although the results of this analysis are not informative as to whether UAMES 29458 is of older

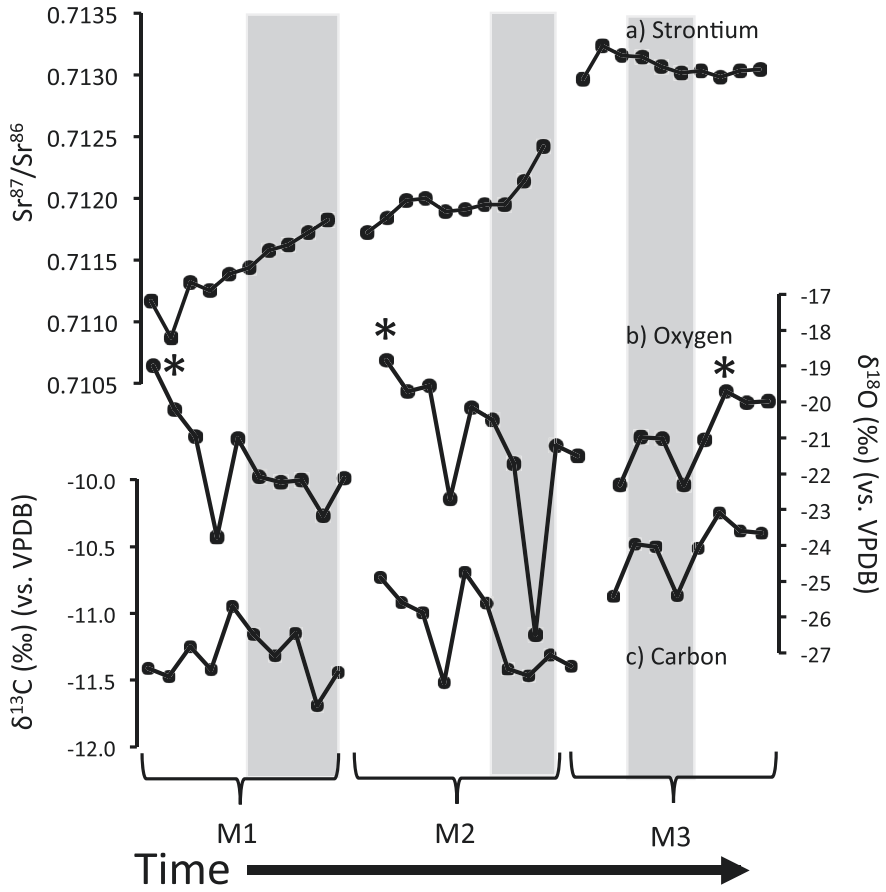

Fig. 7. Isotope data from analyses of molar 1 (M1), molar 2 (M2), and molar 3 (M3) from UAMES 29458. a) Strontium $^{87}Sr/^{86}Sr$ values, b) Oxygen stable isotope ratios expressed as $\delta^{18}O$ values and c) Stable carbon isotope ratios (expressed as $\delta^{13}C$ values). Shading represents estimates of winter, based on the $\delta^{18}O$ values. * Indicate highest $\delta^{18}O$ values associated with summer.

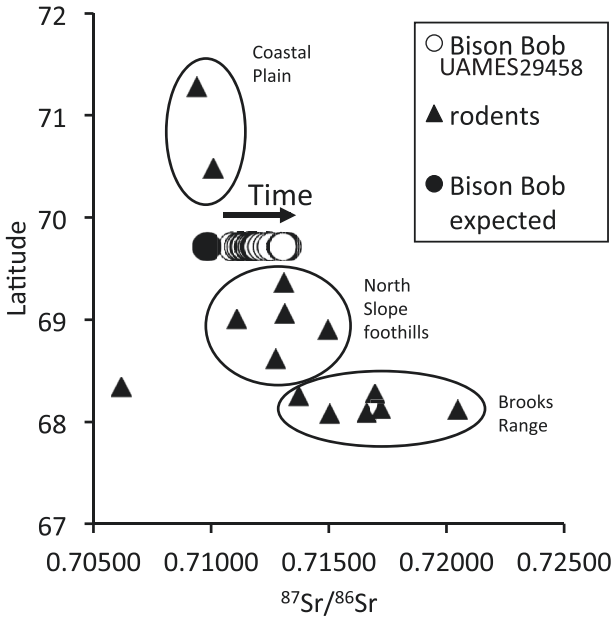

Fig. 8. Rodent $^{87}Sr/^{86}Sr$ values grouped by region, compared to $^{87}Sr/^{86}Sr$ values from UAMES 29458 over time and a model-predicted $^{87}Sr/^{86}Sr$ value for the death location of UAMES 29458.

Table 4
Summary of isotopic results ($\delta^{13}C$‰ and $\delta^{18}O$‰ reported here vs. VPDB).

	Mean	Max	Min	Range
$^{87}Sr/^{86}Sr$	0.71214	0.71324	0.71087	0.00237
$\delta^{13}C$‰	−11.0	−10.3	−11.7	1.5
$\delta^{18}O$‰	−21.2	−18.4	−26.5	8.1

radiocarbon finite or non-finite age, they do suggest that, if the individual were radiocarbon non-finite, it lived after MIS 5e. The finite radiocarbon age from the bison's keratin is within the range of this molecular-clock derived age estimate, which could narrow the age estimate to within MIS 3 (29–57 kya BP). Our phylogenetic analyses show that UAMES 29458 belonged to bison mitochondrial clade 2 (Heintzman et al., 2016). This lineage did not contribute to extant bison diversity, and instead became extinct during the late Holocene, by as long as ~400 years ago (Heintzman et al., 2016; Shapiro et al., 2004). Given the varied methods used for dating this specimen, it is expected that there might be some disagreement between results. However, the two nearly identical dates from the chemically stable portions associated with the specimen (i.e. keratin and insect chitin, 46,000 ± 1100 ^{14}C yr BP and 46,800 ± 1200 ^{14}C yr BP, respectively) provide support for this as a finite-aged specimen very close to the limit of radiocarbon dating. This age is congruent with an appropriate climatic period suggested by the $\delta^{18}O$ values (Fig. 11) and the macrofossil assemblage of flora.

Table 5
Results of the genomic sex determination analysis. X:A ratio is the ratio of the relative mapping frequency of the X chromosome to that of an autosome (1–29, all). Chr.: chromosome. The minimum and maximum X:A ratios are highlighted in bold.

Chr.	Length	Reads mapped	X:A ratio	Chr.	Length	Reads mapped	X:A ratio
1	161428367	10474	0.543	17	76280064	4915	0.547
2	141965563	9334	0.536	18	65811054	4640	0.500
3	126844711	8357	0.535	19	64845320	4500	0.508
4	123809850	8237	0.530	20	75686341	4995	0.534
5	125249322	8237	0.536	21	69078422	4622	0.527
6	122519025	8008	0.539	22	61598339	4384	0.495
7	113029157	7598	0.525	23	52334015	3652	0.505
8	116846264	7802	0.528	24	64508398	4447	0.511
9	108503706	6828	0.560	25	44081797	3137	0.495
10	105982576	7023	0.532	26	51826547	3480	0.525
11	109987751	7605	0.510	27	48460478	3046	**0.561**
12	85119472	5420	0.554	28	45964680	3144	0.516
13	84213851	6029	**0.493**	29	51812796	3432	0.532
14	81216349	5748	0.498	all	2541187220	169841	0.528
15	84472747	5548	0.537				
16	77710258	5199	0.527	X	88654062	3126	NA

4.2. Life history of an individual steppe bison

Multiple lines of evidence suggest that UAMES 29458 was a large bull that was 11–12 years old at the time of death. Present-day male bison of this age are typically lone bulls, either in or just past their prime (Maher and Byers, 1987; Soper, 1941). During his life, this individual incurred injury to a rib and the bone callous clearly indicates it healed (Fig. 3c). This type of injury typically occurs in present-day bison during the rut when bison compete for access to females (Lott, 1971). In addition to this evidence of injury, the early stages of this bison's life, recorded as the $\delta^{15}N$ values from the horn sheath (Fig. 6), could indicate some periods of nutritional stress. Increases in $\delta^{15}N$ values in the tissues of bison can represent stressors, such as starvation, illness, or long-distance movement (Funck et al., 2020). Shifts in $\delta^{15}N$ values are generally used to determine changes in the trophic level (Post, 2002), an interpretation that is not appropriate for a herbivore, except during breast feeding when a juvenile is essentially a trophic level above their mother (Gadbury et al., 2000; Reitsema and Muir, 2015). However, during nutritional stress, such as a hard winter (Funck et al., 2020) or nutritional transition like weaning (Fuller et al., 2003), an animal can break down its muscles to build new proteins, during which tissues fractionate and lead to elevated $\delta^{15}N$ values (Lee et al., 2012). The bison specimen analyzed here exhibited two periods of elevated $\delta^{15}N$ values towards the start of its life (Fig. 6). Horn stubs begin developing in utero but do not solidify into horn spikes until the calves are older (Wiener et al., 2015). The two periods of higher $\delta^{15}N$ values likely occurred in the first 2–3 years of life, overlapping with some of the time periods represented by the molar development, which was used to produce the $\delta^{18}O$ values and $^{87}Sr/^{86}Sr$ ratios. This allows us several lines of evidence for interpreting what early life was like for this bison.

The interpretation of intra-tooth serial samples as a measure of change over time requires an understanding of how teeth develop and mineralize. For example, the molars of bison have been shown to grow over 2–2.5 years (Gadbury et al., 2000; Higgins and MacFadden, 2004; Velivetskaya et al., 2016) and the pattern of molar eruption occurs in a particular sequence and time in an animal's life. As each molar develops, discrete layers of enamel are laid down and retain the isotopic composition of conditions at each point in time. However, as a tooth develops it continues to mineralize over 6–7 months leading to a degree of isotopic averaging (Balasse, 2002; Montgomery et al., 2010). As a result, changes that may appear progressive could in fact occur over much shorter periods of time and the exact timing of tooth development and mineralization can be subject to some degree of variation between individuals and species. However, Velivetskaya et al. (2016) used high-resolution sampling for analysis of $\delta^{18}O$ values to pinpoint the timing of tooth development in two late-Pleistocene steppe bison from the Middle Urals, Russia and found it to be close to those of present-day bison. Seasonal oscillation in $\delta^{18}O$ values can also be compared to those of present-day animals to track the speed of tooth development.

The M1 is formed in utero and shortly after birth (Bernard et al., 2009; Widga et al., 2010), and thus represents the mother's home range and the calving grounds. The M1 formation likely corresponds with the timing of the first $\delta^{15}N$ value peak (Fig. 6). The $^{87}Sr/^{86}Sr$ ratios from the M1 had less variation than the M2 suggesting the mother remained in a relatively consistent geological area. When the M1 $^{87}Sr/^{86}Sr$ values are compared to bioavailable $^{87}Sr/^{86}Sr$ ratios from the region, it appears that this bison began life on the Alaska coastal plain (Fig. 8). Contemporary caribou from similar regions of Alaska currently use the coastal plain as calving grounds, taking advantage of the emerging graminoids and open terrain (Fancy et al., 1990; Post and Forchhammer, 2008). Subsequently, they move to higher ground to avoid insects and to take advantage of abundant lichens that sustain them during non-calving seasons (Fancy et al., 1990). Bison calves are dependent on milk for the first ~5 months and gradually stop suckling over 9–21 months (Green et al., 1993). So the first peak in $\delta^{15}N$ values from the horn (Fig. 6) likely corresponds to this M1 period and could be interpreted as a maternal/weaning signal (Gadbury et al., 2000; Reitsema and Muir, 2015), either attributed to the bison being at a higher trophic level than its mother from which it was nursing, or the effect of weaning and the nutritional stress that it may have imparted (Fuller et al., 2003).

After the period of initial relative geographic stability inferred from the $^{87}Sr/^{86}Sr$ ratios in the M1, which likely represented the first half-year of life, the bison seems to have dispersed into a new geographic area during its second summer according to the $^{87}Sr/^{86}Sr$ ratios from the M2 and M3. The M2 development starts at ~2–3 months of age and continues for 12–15 months (Gadbury et al., 2000; Velivetskaya et al., 2016). The M3 subsequently develops from the beginning of the second summer after weaning, ~10–11 months until the age of about 2–2.5 years (Gadbury et al., 2000; Velivetskaya et al., 2016). Comparisons of the bison's $^{87}Sr/^{86}Sr$ ratios from the M2 and M3 to bioavailable $^{87}Sr/^{86}Sr$ ratios from the region indicate that the bison may have moved into the foothills of the Brooks Range (Figs. 1 and 8). The second peak in $\delta^{15}N$ values from the analyses of the horn sheath (Fig. 6) could correspond to

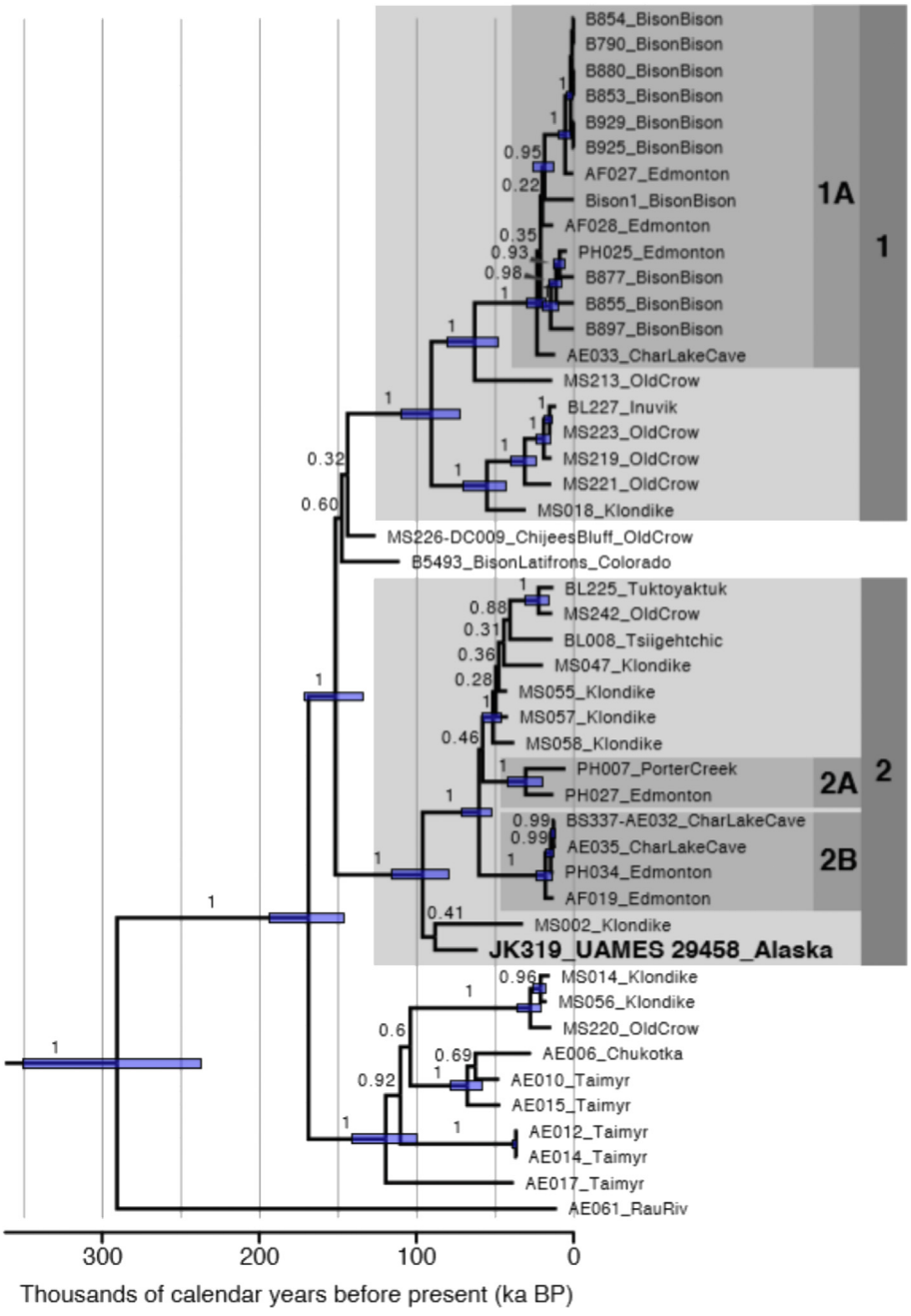

Fig. 9. A Bayesian time-calibrated genealogy of bison mitochondrial genomes, with major well-supported Clades (1, 1 A, 2, 2 A, 2 B) highlighted (following Heintzman et al., 2016 and Zazula et al., 2017). All living bison fall within Clade 1 A, whereas the UAMES 29458 falls near the base of Clade 2. Purple bars are 95% highest posterior density intervals for node heights and are shown for nodes with posterior probability >0.95. This maximum clade credibility tree resulted from the analysis that excluded MS022 and had a minimum age prior of 30 kya BP for UAMES 29458. Results from the other analyses can be found in Table 6. The diverged yak tips have been removed.

mobility on the landscape, which seems to have occurred during this period. A study on present-day wood bison in Alaska (Funck et al., 2020) found that bison that traveled long distances, or experienced nutritional stress, produced elevated $\delta^{15}N$ values due to the energetic costs of travel. The horn $\delta^{13}C$ record begins relatively low shortly before this point, which could be related to the bison beginning to draw on the bodies lipids which have lower $\delta^{13}C$ values (DeNiro and Epstein, 1977; Rode et al., 2018). This offset follows the same pattern found in a modern wood bison experiencing a dispersal related dietary stress (Funck et al., 2020). In the present study, the tooth carbonate $\delta^{13}C$ values show an overall increase (+1‰) during this same period (~2.5 years), consistent with a change from a wetter environment to a drier one (Wooller et al., 2007), which also seems to correspond with a shift towards the higher and drier elevations of the foothills compared to the wetter, lower reaches, of the coastal plain. Later in the bison's life, after the record preserved in the molars is fully mineralized (~2.5 years), we lose track of the specimen's geolocation based on the $^{87}Sr/^{86}Sr$ record. However, this bison must have eventually returned to the coastal plain to the location where he eventually died and was found (Fig. 1).

In contrast to the tooth record, the horn sheath continues to

Table 6
Summary of the Bayesian molecular analyses of JK319/UAMES 29458, with overall maximum age ranges highlighted in bold.

Analysis variables		Phylogenetic placement		Estimated age		
Min. age prior	MS022	Placement	Posterior probability	Minimum	Maximum	ESS
0	Included	1	0.276	**32,653**	85,157	11376
0	Excluded	1	0.410	36,022	**86,643**	20465
20,000	Included	1	0.261	34,300	85,618	15546
20,000	Excluded	1	0.409	34,929	85,827	18525
30,000	Included	1	0.268	34,708	83,346	19814
30,000	Excluded	1	0.407	36,696	85,376	18945
40,000	Included	1	0.241	40,021	81,074	19367
40,000	Excluded	1	0.391	40,227	82,423	19013
50,000	Included	2	0.678	50,000	82,285	20687
50,000	Excluded	2	1.000	50,007	82,935	18967

Phylogenetic placements are: 1) sister to MS002, and 2) at the base of Clade 2 (see Fig. 9). Minimum and maximum ages are based on 95% highest posterior density credibility intervals. Note that, for analyses with a minimum age prior of 40 and 50 kya BP, the estimated minimum ages are likely to have been truncated by the prior. ESS: estimated sample size.

develop over approximately the lifetime of the individual. The $\delta^{15}N$ fluctuates through what appear to be seasonal oscillations of slightly more elevated $\delta^{15}N$ values in the winter, likely due to nutritional stress during this season, then lower $\delta^{15}N$ values during more favorable summers, interpreted based on isotopic patterns exhibited in present-day bison from Alaska (Funck et al., 2020). Present-day wood bison south of the Brooks Range in Alaska only had changes in $\delta^{15}N$ values during particularly hard winters (Funck et al., 2020). Thus, these winters were likely harder than the conditions experienced by present-day analogous populations. Applying this seasonal pattern implies that the sample closest to the horn core (i.e. the period leading to the animal's death) represented the start of the transition from the summer to winter. This indicates that the bison was not experiencing unusual nutritional stress and did not appear to have been in a weakened state prior to death. Other potential causes for changes in $\delta^{15}N$ values in herbivores could include changes in the seasonal $\delta^{15}N$ values of forage and seasonal movement to regions with very different baseline $\delta^{15}N$ values. Our data indicates that this bison individual did move substantially across the landscape. However, the tooth record of paleomobility is not long enough to cover the longer record represented by the horn sheath data. We find that our interpretation of the $\delta^{15}N$ values as a marker in terms of changes in the degree of nutritional stress is in some ways supported by the $\delta^{13}C$ data from the horn sheath. For example, the low $\delta^{13}C$ values from the horn sheath in the last year of life, relative to the rest of the record from the horn, could indicate that the animal may have begun to draw on its lipid reserves (Funck et al., 2020). Although in some animals these isotopic shifts occurs only at extreme thresholds of starvation this is a more common strategy in animals that have large fat and muscle reserves for winter use, such as bison (Funck et al., 2020).

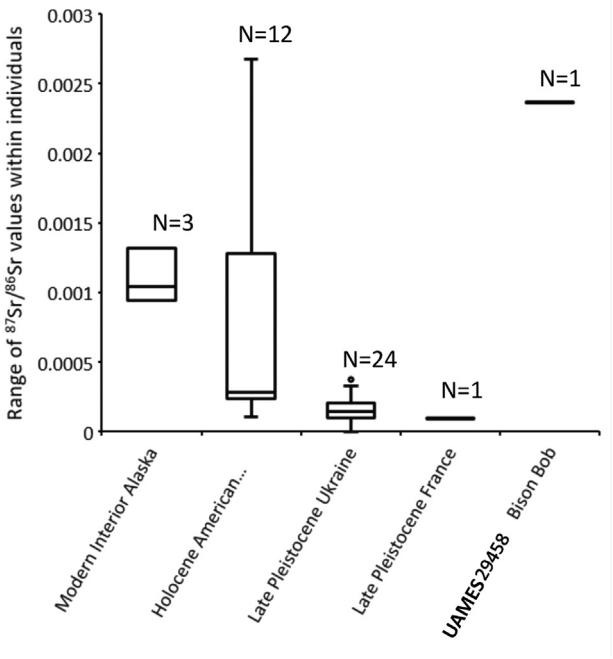

Fig. 10. Comparison of the ranges (Δ) of $^{87}Sr/^{86}Sr$ values recorded within the teeth of different bison including, present-day plains bison (*Bison bison*) from interior Alaska (Glassburn et al., 2018); Holocene plains bison (*Bison bison*) from the American Plains (Widga et al., 2010); Late Pleistocene steppe bison (*Bison priscus*) from Ukraine (Julien et al., 2012) and Late Pleistocene steppe bison (*Bison priscus*) from France (Britton et al., 2011).

The degree of mobility of the bison specimen analyzed, based on the $^{87}Sr/^{86}Sr$ data from the North Slope specimen, is relatively high compared to data from other ancient and present-day bison (Fig. 10, Table 7; Britton et al., 2011; Glassburn et al., 2015; Julien et al., 2012; Widga et al., 2010). Although the range of $^{87}Sr/^{86}Sr$ ratios cannot be directly compared, because variability is highly dependent on the geological heterogeneity of a landscape that individuals inhabit, it is worth considering this bison in the context of others analyzed using the similar methods. Britton et al. (2011) examined a single bison from western France dating to 49,000 ± 5000 BP and demonstrated high fidelity to an area, with almost no variability in $^{87}Sr/^{86}Sr$ values despite a variable geological environment. Julien et al. (2012) found that steppe bison from the Last Glacial Maximum (LGM) (~20.5 kya BP) in Amrosievika in Eastern Ukraine had a $^{87}Sr/^{86}Sr$ range of 0.00074 (Julien et al., 2012). This range was attributed to the low degree of variability to minimal mobility on the landscape because there was no signal from mixed geology as close as 20 km to the south-west of the site where the bison were found (Julien et al., 2012). A study of bison herds on the Great Plains of North America from the Middle Holocene indicated that bison also had limited seasonal mobility (<50 km), while inter-annual movement of herds over ~4–5 yrs moved further afield (<500 km) (Widga et al., 2010a). In contrast, present-day *Bison bison* from the interior of Alaska, with an observed seasonal and regional migration route of about a 100 km, had $^{87}Sr/^{86}Sr$ ratio range from 0.71714 to 0.71540 (0.00174) (Glassburn et al., 2018). Although these regions and studies cannot be quantitatively compared because of difference in local geology (Bataille et al., 2020) we can still draw some qualitative comparisons. The variability in $^{87}Sr/^{86}Sr$ ranges among bison from different localities and periods suggests that bison utilize different mobility strategies that

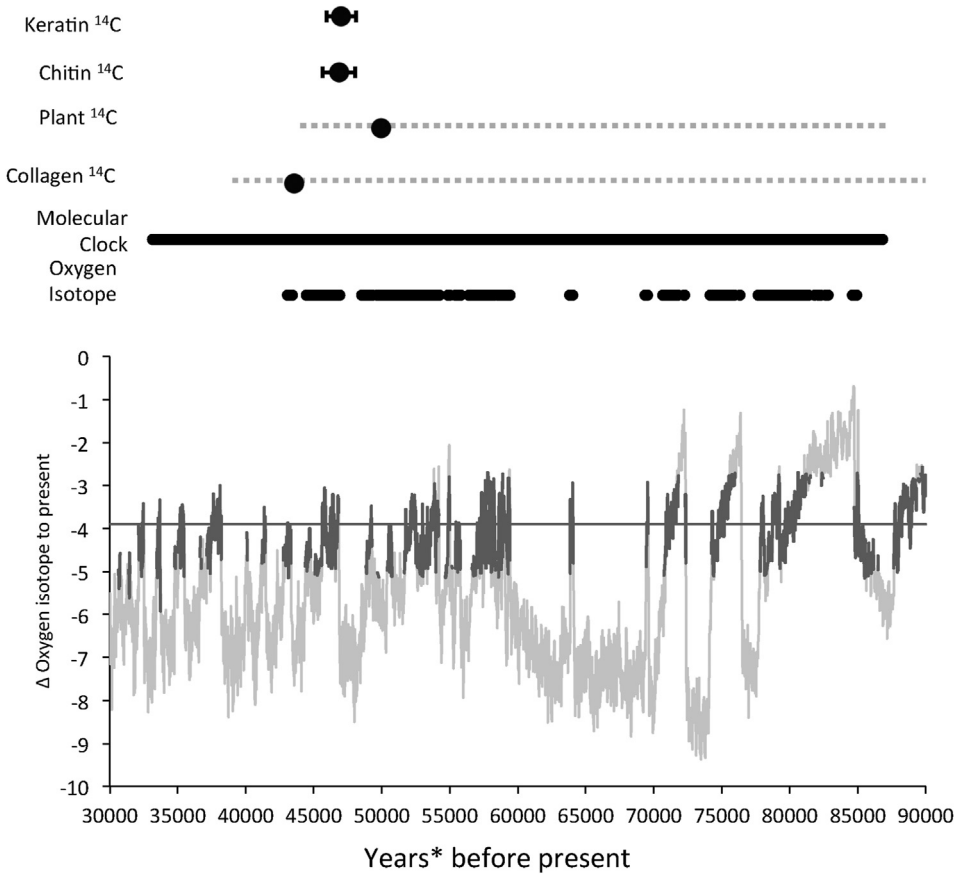

Fig. 11. Summary of all radiocarbon dates (^{14}C), molecular clock estimates, and compatible $\delta^{18}O$ value periods based on Greenland Ice core values (Rasmussen et al., 2014) and a Δ4‰ lower values than present. *dates are calibrated radiocarbon dates where possible, otherwise they are before present.

Table 7
Comparison to other Bison strontium data. See Fig. 10 *Stratigraphically determined to be from MIS4 **Molecular clock.

Context	Species	N	Date	Average Range	Citation
Present-day Interior Alaska	*Bison bison*	3	2014	0.00111	Glassburn et al. (2018)
Holocene American Plaines	*Bison bison*	12	8930-6980 cal yr BP	0.00077	Widga et al. (2010)
Late Pleistocene Ukraine	*Bison priscus*	24	20557-20,491 cal yr BP	0.00016	Julien et al. (2012)
Late Pleistocene France	*Bison priscus*	1	49,000 ± 5 yr BP*	0.00010	Britton et al. (2011)
Bison Bob	*Bison priscus*	1	33-87,000 yr BP**	0.00237	This paper

are dependent on (paleo)ecological conditions. The range of $^{87}Sr/^{86}Sr$ variation from the North Slope bison specimen analyzed here (0.00237) is relatively large compared to all these previous measures, indicating that he was likely a gregarious individual who traveled some distance during his early years of life. There is a large geological range in this region (Bataille et al., 2020) that this bison appears to be utilizing. Future research could integrate genetic testing of sex from specimens to determine if males and females used different mobility strategies.

4.3. Necrology and biostratinomy

Evidence from UAMES 29458 helps shape a paleoecological picture leading up to the individual's death, decomposition, and the mechanism of burial. The bones from the bison specimen were overall in a state of excellent preservation as evidenced by the presence of intact horn, hooves, fur, spinal cord, cartilage, and possible brain tissues. Specimens of this level of completeness are extremely rare in Quaternary deposits. There were no obvious signs of the cause of death, such as bite marks around the nose or neck, and all carnivore marks were related to scavenging (Andersson et al., 2011) but predation cannot be ruled out. After death, the specimen came to finally rest on his right side, which protected that side from scavenging. This is further supported by the presence of vivianite. Vivianite deposits tend- to be on the bone surfaces that were exposed to the ground surface and root etching also tends to be present on the surfaces of the bones that rested on the ground (Supplemental data).

Carnivore tooth marks are present at various locations on the specimen, indicating that scavenging of the bison carcass occurred post mortem (Fig. 3 a and b and Supplemental data). There are four major carnivore taxa present contemporaneously that could cause the type of damage seen on UAMES 29458: *Arctodus simus* (short-faced bear), *Canis lupus* (wolf), *Homotherium serum* (scimitar cat), and *Panthera atrox* (American lion) (Fox-dobbs et al., 2008; Schubert, 2010). The dentition marks (Fig. 3) are consistently narrow punctures, which are not consistent with the wide teeth of *A. simus* (Sorkin, 2006) or *H. serum* (Ewald et al., 2018). The incisor

punctures indicated that the space between the canines is at least 6 cm apart (Fig. 3a, which is consistent with *P. atrox* (Baryshnikov and Boeskorov, 2001; Christiansen and Harris, 2010). This may be out of the range of the smaller *C. lupus* (Sorkin, 2006), leaving large felids as the most likely scavenger. Further analysis of dentition morphometrics in predator species would be useful for this type of taphonomic analysis. Indication of lion scavenging have also been found on other preserved bison specimens from in Alaska (Guthrie, 1989). It is likely that only one individual scavenger caused all of the damage based on the consistency in size of the tooth marks of the 14 tooth marks with punctures. The 11 instances of gnawing are less diagnostic but also appear consistent. The limited scavenging also supports a single scavenger, as more individuals would require less time to remove meat, disarticulate the corpse, and scavenge from a greater area of the carcass (Blumenschine, 1986). The carnivore appears to have consumed the bison carcass and ate portions of the backstrap (meat along the top of the spine) based on observed damage along the spinous processes of several vertebrae (Fig. 3 a and b). The carnivore also seems to have consumed the carcass from the inside of the body and likely ate the internal organs and tenderloin based on damage to the costal cartilage, the distal ribs, the transverse processes of the lumbar vertebrae, and the sacrum. In addition, the carnivore gnawed the left humerus and likely removed the left scapula, in an attempt to get at the flesh of the left fore-limb. Scavenging only seems to have occurred in high-value areas, supporting an inference that the carcass was likely buried rapidly. In most contexts a carcass on an open landscape with carnivores can be consumed and disarticulated within hours to a few days (Blumenschine, 1986). It is for this reason that complete specimens are extremely rare. Thus, for this specimen to preserve, something exceptional must have occurred to protect it. During the erosion that re-exposed the bison it seems the left extremities of the front and hind limbs (phalanxes, carpals, tarsals, etc.) may have been lost due to erosional processes (Fig. 2). These skeletal elements would be the first to be exposed and vulnerable to gravity, weathering, and would have been preferentially removed via taphonomic agents (e.g., eroded into the river and lost). These skeletal elements of the lower extremities are also not associated with high food value flesh and likely would not have been a target for scavenging.

The presence of the blow fly puparia recovered from inside the skull made it possible to propose some “paleoforensic” hypotheses associated with postmortem events. Blow flies figure among the most relevant witnesses in forensic entomology in order to determine the time elapsed since death, namely the postmortem interval (PMI) because blow flies (Calliphoridae) are the first and predominant organisms to colonize a body after death. Within hours of death, these insects are attracted to the smell of the decomposing remains, which are both a site for laying eggs and a source of protein for larval development. Under normal circumstances, egg laying occurs soon after death (1–3 days) (Gomes et al., 2006). The favored egg-laying sites are the natural openings of the body (mouth, eyes, anus) as well as any wounds present on the corpse (Gomes et al., 2006). The species preserved on the carcass *Protophormia terraenovae* (Robineau Desvoidy) is a Holarctic, cold-adapted species, present throughout northern Europe and Asia. Very common in the cooler high latitude regions and notably in the Arctic, representatives of this species are found within 890 km of the North Pole (Smith, 1986). Experiments conducted by Marchenko (2001) found that the development period of *P. terraenovae* (from egg to adult) is relatively long. According to Warren and Anderson (2013), egg-carrying females of *P. terraenovae* do not lay eggs at temperatures lower than 10.3 °C. In the North Slope region, temperatures only reach above 10 °C during the summer period (https://www.weatherbase.com). Insects, like all arthropods, are coldblooded and the duration of their life-cycle is primarily temperature driven. Rate of development is species-specific and influenced by biotic (e.g. maggot mass that can significantly accelerate rate of development) and environmental factors (exposure of the carcass to sunlight or shade, rain, and wind). Following the biological data provided by Marchenko (2001), and focusing on temperatures ranging from 11 to 18 °C (respectively the average minimal temperature required for laying eggs and the current maximum temperatures recorded on the paleontological site), *P. terraenovae* development extends from 15 to 50 days (egg to pupal stage) and adult emergence from 24 to 78 days. In the case of UAMES 29458, all of the puparia were intact with no evidence of adult emergence.

The fact that the bison’s skeleton was almost complete and articulated, and not fully scavenged by carnivores suggests that the fly pupal stage intervened fairly quickly, indicating relatively high temperatures at the time of death (e.g., at 18 °C, the pupal stage would have started on the 15th day). The bison carcass was then quickly covered with sediment or snow precluding further access to predators; however, a few centimeters of soil cover would not prevent the development and emergence of flies (Balme et al., 2012). Trapped in the skull, the pupae would have preserved in situ. The presence of unhatched fly puparia of *P. terraenovae* recovered from the bison individual would suggest that its carcass had been subaerially exposed for at least 2 weeks before the life cycle was interrupted either due to a more complete burial or freezing. The fact that the carcass was little affected by scavengers over this period might be explain by low scavenger density on site, high carcass availability or because the bison’s remains were only accessible to flying insects and not by terrestrial scavengers (e.g. carcass partially exposed in river water). Finally, we can argue that the ambient temperature was very likely over 10 °C when the fly infestation occurred, requiring the events to occur during a warm period of the year. This warm period seems to have been at the transition from summer to winter, based on the isotopic evidence from the horn sheath.

Fluvial sediments including plant macrofossils likely entered the skull after this initial burial during which the *P. terraenovae* puparia developed. The plant macrofossils recovered from inside the skull and neural canal are unlikely penecontemporaneous with the death of this bison individual, but could indicate an overall glimpse of the surroundings. The macrofossil assemblage of plants is consistent with an Arctic flood plain. The immediate surrounding of the river was probably covered in moss, low shrubs, and bogs (Fig. 5). Further away from the banks of the river were likely drier tundra with grasses, sedges, and a variety of tundra flowers including *Papaver* sp., *Polygonum bistorta,* and *Draba* type (Fig. 5). Overall, the plant assemblage is more typical of a mesic tundra than a steppe and possibly originated from an inter-glacial or interstadial environment (Gaglioti et al., 2018).

Overall, we conclude that this bison died on a flood plain during the warm period prior to the onset of winter and fell on to its right side. A carnivore, possibly a large felid, quickly consumed high-value areas of meat and blow flies swiftly laid eggs within the skull. Alluvial sediments or possibly snow then quickly buried the carcass before the carcass could be further disarticulated. At least two weeks passed before temperatures inside the carcass or the oxygen availability fell too low for the puparia to continue developing.

5. Conclusion

Our multi-proxy paleoecological evidence from UAMES 29458 fills out the details of an individual bison’s life and death in the Arctic, where bison were once a dominant herbivore. Combining

serial isotope analyses with aDNA allowed us to combine mobility information with genealogical information, and to place the individual within bison meta-population dynamics over millennia. This augments a paleoecological picture based on the physical evidence of the skeletal remains alone, providing a more vivid image of a highly mobile individual moving across the North Slope of Alaska. The mitochondrial lineage of this bison is one that thrived in Beringia but ultimately died out. Our multiproxy evaluation indicates that this bison likely lived during an interstadial period, which in some ways may have been somewhat similar to today. Strontium isotope data from the specimen indicates that he dispersed across the Northern Alaska landscape from possible calving grounds located on the Arctic coastal plain to the foothills of the Brooks Range in early life and ultimately back to his place of death on the Arctic coastal plain. Nitrogen isotopes from the horn sheath indicate that the mobility of his early life may have resulted in significant nutritional stress, and that this individual suffered somewhat harsher winters than those on the North Slope today. The taphonomic analysis revealed that this bison was scavenged in parts of high nutritional value, which was followed by a rapid burial in a riverine environment. In this case, a multiproxy approach has uncovered a life history and detailed examination of a member of a dominant Pleistocene species in the Arctic.

Author statement

All of the authors contributed to the interpretation of data in the paper and the writing of the manuscript.

Declaration of competing interest

None of the authors have any conflict of interests.

Acknowledgments

First and foremost, we recognize and are very grateful for the efforts of Dr. Dannial Mann and Dr. Pamela Groves in discovering, excavating, and transporting this exceptional specimen, affectionately known as 'Bison Bob' to the UAM. Without them none of this work would have been possible and we thank them for discussions. The bison specimen was collected during fieldwork directed by Mike Kunz and funded by the Bureau of Land Management. Kathrine Anderson in the UAM Earth Sciences Collection managed curation of the bison specimen. In addition, she assisted Stormy Fields and Juliette Funck in preparing the specimen for taphonomic analysis. Aren Gunderson helped locate and select rodent specimens in the UAM Mammalogy Collection. Dr. Diego Fernandez at the University of Utah conducted strontium isotope analysis. We thank Tim Howe at the Alaska Stable Isotope Facility for assistance conducting the stable isotope analyses of the specimen. Amanda Barker provided support and advice on chemistry preparation. Radiocarbon analysis was conducted by W. M. Keck Carbon Cycle Accelerator Mass Spectrometry Laboratory by Dr. John Southon, who provided expertise in evaluating radiocarbon results from the bison specimen. The Bureau of Land Management (USA) oversaw specimen management and permitted destructive analysis of necessary materials for this study. The 2016, 2017 David and Rachel Hopkins Fellowship (USA) provided funds for strontium analysis. Dr. Beth Shapiro was supported by IMLS MG-30-17-0045-17 (USA). Gemma Murray and Dr. Peter Heintzman were partially supported by NSF DEB 1754451 (USA). Joshua D. Kapp assisted in the aDNA analysis. Dr. Derek Sikes, Dr. Denise Gemmellaro, and Dr. Martin Hall were all contacted for their expertise with forensic entomology. We thank two anonymous reviewers for their constructive input that improved this research.

Appendix A. Supplementary data

Supplementary data to this article can be found online at https://doi.org/10.1016/j.quascirev.2020.106578.

References

Andersson, K., Norman, D., Werdelin, L., 2011. Sabretoothed carnivores and the killing of large prey. PloS One 6, 8–13. https://doi.org/10.1371/journal.pone.0024971.

Balasse, M., 2002. Reconstructing dietary and environmental history from enamel isotopic analysis: time resolution of intra-tooth sequential sampling. Int. J. Osteoarchaeol. 12, 155–165. https://doi.org/10.1002/oa.601.

Balasse, M., Bocherens, H., Mariotti, A., Ambrose, S.H., 2001. Detection of dietary changes by intra-tooth carbon and nitrogen isotopic analysis: an experimental study of dentine collagen of cattle (*Bos taurus*). J. Archaeol. Sci. 28, 235–245. https://doi.org/10.1006/jasc.1999.0535.

Balme, G.R., Denning, S.S., Cammack, J.A., Watson, D.W., 2012. Blow flies (Diptera: calliphoridae) survive burial: evidence of ascending vertical dispersal. Forensic Sci. Int. 216, e1–e4. https://doi.org/10.1016/j.forsciint.2011.07.017.

Bamforth, D.B., 1987. Historical documents and Bison ecology on the Great plains. Plains Antrhoplogist 32, 1–16. https://doi.org/10.1080/2052546.1987.11909364.

Barbosa, I.C.R., Kley, M., Schaufele, R., Auerswald, K., Schroder, W., Filli, F., Hertwig, S., Schnyder, H., 2009. Analysing the isotopic life history of the alpine ungulates *Capra ibex* and *Rupicapra rupicapra rupicapra* through their horns. Rapid Commun. Mass Spectrom. 23, 2347–2356. https://doi.org/10.1002/rcm.

Baryshnikov, G., Boeskorov, G., 2001. The pleistocene cave lion, Panthera spelaea (Carnivora, Felidae) from Yakutia, Russia. CRANIUM 18.

Bataille, C.P., Bowen, G.J., 2012. Sr/86 Sr variations in bedrock and water for large scale provenance studies. Chem. Geol. 304–305, 39–52. https://doi.org/10.1016/j.chemgeo.2012.01.028.

Bataille, C.P., Brennan, S.R., Hartmann, J., Moosdorf, N., Wooller, M.J., Bowen, G.J., 2014. A geostatistical framework for predicting variability in strontium concentrations and isotope ratios in Alaskan rivers. Chem. Geol. 389, 1–15. https://doi.org/10.1016/j.chemgeo.2014.08.030.

Bataille, C.P., Crowley, B.E., Wooller, M.J., Bowen, G.J., 2020. Advances in global bioavailable strontium isoscapes. Palaeogeogr. Palaeoclimatol. Palaeoecol. 555, 109849. https://doi.org/10.1016/j.palaeo.2020.109849.

Berger, J., 2004. The last mile: how to sustain long-distance migration in mammals. Conserv. Biol. 18, 320–331. https://doi.org/10.1111/j.1523-1739.2004.00548.x.

Bernard, A., Daux, V., Lécuyer, C., Brugal, J.P., Genty, D., Wainer, K., Gardien, V., Fourel, F., Jaubert, J., 2009. Pleistocene seasonal temperature variations recorded in the $\delta^{18}O$ of *Bison priscus* teeth. Earth Planet Sci. Lett. 283, 133–143. https://doi.org/10.1016/j.epsl.2009.04.005.

Bigelow, N.H., Zazula, G.D., Atkinson, D.E., 2013. Plant macrofossil records: arctic north America. In: Elias, S.A., Mock, C.J. (Eds.), Encyclopedia of Quaternary Science. Elsevier, Amsterdam, pp. 746–759.

Binford, L.R., 1981. Bones: Ancient Men, Modern Myths. Academic Press, New York.

Blumenschine, R.J., 1986. Carcass consumption sequences and the archaeological distinction of scavenging and hunting. J. Hum. Evol. 15, 639–659. https://doi.org/10.1016/S0047-2484(86)80002-1.

Bocherens, H., 2003. Isotopic biogeochemistry and the paleoecology of the mammoth steppe fauna. In: Reumer, J. (Ed.), Advances in Mammoth Research, Proceedings of the 2nd International Mammoth Conference, vol. 9. DEINSEA, Rotterdam, pp. 57–76.

Boeskorov, G.G., Potapova, O.R., Protopopov, A.V., Plotnikov, V.V., Agenbroad, L.D., Kirikov, K.S., Pavlov, I.S., Shchelchkova, M.V., Belolyubskii, I.N., Tomshin, M.D., Kowalczyk, R., Davydov, S.P., Kolesov, S.D., Tikhonov, A.N., van der Plicht, J., 2016. The Yukagir Bison: the exterior morphology of a complete frozen mummy of the extinct steppe bison, *Bison priscus* from the early Holocene of northern Yakutia, Russia. Quat. Int. 406, 94–110. https://doi.org/10.1016/j.quaint.2015.11.084.

Bousquet, Y., Bouchard, P., Davies, A.E., Sikes, D.S., 2013. Checklist of beetles (Coleoptera) of Canada and Alaska. ZooKeys 44, 1–44. https://doi.org/10.3897/zookeys.360.4742 second ed.

Bowen, G.J., 2018. WaterIsotopes.org [WWW Document]. Univ. Utah. Accessed: Dec. 2019.

Brennan, S.R., Fernandez, D.P., Mackey, G., Cerling, T.E., Bataille, C.P., Bowen, G.J., Wooller, M.J., 2014. Strontium isotope variation and carbonate versus silicate weathering in rivers from across Alaska: implications for provenance studies. Chem. Geol. 389, 167–181. https://doi.org/10.1016/j.chemgeo.2014.08.018.

Briggs, A.W., Good, J.M., Green, R.E., Krause, J., Maricic, T., Stenzel, U., Lalueza-fox, C., Rudan, P., Brajković, D., Kućan, Ž., Rasilla, M. De, Fortea, J., Rosas, A., Pääbo, S., 2009. Five neandertal mtDNA genomes. Science (80-.) 325, 318–321.

Britton, K., 2009. Reconstructing faunal migrations using intra- tooth sampling and strontium and oxygen isotope analyses : a case study of modern caribou (Rangifer tarandus granti). https://doi.org/10.1016/j.jas.2009.01.003.

Britton, K., Gaudzinski-Windheuser, S., Roebroeks, W., Kindler, L., Richards, M.P., 2012. Stable isotope analysis of well-preserved 120,000-year-old herbivore bone collagen from the Middle Palaeolithic site of Neumark-Nord 2, Germany reveals niche separation between bovids and equids. Palaeogeogr. Palaeoclimatol. Palaeoecol. 333–334, 168–177. https://doi.org/10.1016/j.palaeo.2012.03.028.

Britton, K., Grimes, V., Dau, J., Richards, M.P., 2009. Reconstructing faunal migrations using intra-tooth sampling and strontium and oxygen isotope analyses: a case study of modern caribou (*Rangifer tarandus granti*). J. Archaeol. Sci. 36, 1163–1172. https://doi.org/10.1016/j.jas.2009.01.003.

Britton, K., Grimes, V., Niven, L., Steele, T.E., McPherron, S., Soressi, M., Kelly, T.E., Jaubert, J., Hublin, J.J., Richards, M.P., 2011. Strontium isotope evidence for migration in late Pleistocene Rangifer: implications for Neanderthal hunting strategies at the Middle Palaeolithic site of Jonzac, France. J. Hum. Evol. 61, 176–185. https://doi.org/10.1016/j.jhevol.2011.03.004.

Capo, R.C., Stewart, B.W., Chadwick, O.A., 1998. Strontium isotopes as tracers of ecosystem processes: theory and methods. Geoderma 82 (21), 197–225. https://doi.org/10.1016/S0016-7061(97)00102-X.

Carlson, K., Bement, L.C., Carter, B.J., Culleton, B.J., Kennett, D.J., 2016. A Younger Dryas signature in bison bone stable isotopes from the southern Plains of North America. J. Archaeol. Sci. Reports 1–7. https://doi.org/10.1016/j.jasrep.2017.03.001.

Carter, L.D., 1981. A pleistocene sand sea on the alaskan arctic coastal plain. Science 211, 381–383. https://doi.org/10.1126/science.211.4480.381.

Cerling, T.E., Harris, J.M., 1999. Carbon isotope fractionation between diet and bioapatite in ungulate mammals and implications for ecological and paleoecological studies. Oecologia 120, 347–363. https://doi.org/10.1007/s004420050868.

Christiansen, P., Harris, J.M., 2010. Craniomandibular morphology and phylogenetic affinities of *Panthera atrox*: implications for the evolution and paleobiology of the lion lineage. J. Vertebr. Paelontology 4634. https://doi.org/10.1671/039.029.0314.

Clark, P.U., Dyke, A.S., Shakun, J.D., Carlson, A.E., Clark, J., Wohlfarth, B., Mitrovica, J.X., Hostetler, S.W., McCabe, A.M., 2009. The last glacial maximum. Science (80- 325, 710–714. https://doi.org/10.1126/science.1172873.

Cody, W.J., 2000. Flora of the Yukon Territory, second ed. NRC Research Press, Ottawa, Ontario, Canada.

Dabney, J., Knapp, M., Glocke, I., Gansauge, M.-T., Weihmann, A., Nickel, B., Valdiosera, C., Garcia, N., Paabo, S., Arsuaga, J.-L., Meyer, M., 2013. Complete mitochondrial genome sequence of a Middle Pleistocene cave bear reconstructed from ultrashort DNA fragments. Proc. Natl. Acad. Sci. Unit. States Am. 110, 15758–15763. https://doi.org/10.1073/pnas.1314445110.

Delgiudice, G.D., Kerr, K.D., Mech, L.D., Seal, U.S., 2000. Prolonged winter undernutrition and the interpretation of urinary allantoin : creatinine ratios in white-tailed deer. Can. J. Zool. 78, 2147–2155.

DeNiro, M.J., Epstein, S., 1977. Mechanism of carbon isotope fractionation associated with lipid synthesis. Am. Assoc. Adv. Sci. 197, 261–263.

Domínguez-Rodrigo, M., 1999. Flesh availability and bone modifications in carcasses consumed by lions: palaeoecological relevance in hominid foraging patterns. Palaeogeogr. Palaeoclimatol. Palaeoecol. 149, 373–388. https://doi.org/10.1016/S0031-0182(98)00213-2.

Drucker, D., Bocherens, H., Bridault, A., Billiou, D., 2003. Carbon and nitrogen isotopic composition of red deer (*Cervus elaphus*) collagen as a tool for tracking palaeoenvironmental change during the Late-Glacial and Early Holocene in the northern Jura (France). Palaeogeogr. Palaeoclimatol. Palaeoecol. 195, 375–388. https://doi.org/10.1016/S0031-0182(03)00366-3.

Drucker, D.G., Bridault, A., Hobson, K.a., Szuma, E., Bocherens, H., 2008. Can carbon-13 in large herbivores reflect the canopy effect in temperate and boreal ecosystems? Evidence from modern and ancient ungulates. Palaeogeogr. Palaeoclimatol. Palaeoecol. 266, 69–82. https://doi.org/10.1016/j.palaeo.2008.03.020.

Drucker, D.G., Hobson, K. a, Ouellet, J.-P., Courtois, R., 2010. Influence of forage preferences and habitat use on ^{13}C and ^{15}N abundance in wild caribou (*Rangifer tarandus* caribou) and moose (*Alces alces*) from Canada. Isot. Environ. Health Stud. 46, 107–121. https://doi.org/10.1080/10256010903388410.

Drummond, A.J., Suchard, M.A., Xie, D., Rambaut, A., 2012. Bayesian phylogenetics with BEAUti and the BEAST 1.7. Mol. Biol. Evol. 29, 1969–1973. https://doi.org/10.1093/molbev/mss075.

Elias, S.A., Berman, D., Alfimov, A., 2000. Late pleistocene beetle faunas of beringia: where east met west. J. Biogeogr. 27, 1349–1363. https://doi.org/10.1046/j.1365-2699.2000.00503.x.

Elias, S.A., Crocker, B., 2008. The Bering Land Bridge: a moisture barrier to the dispersal of steppe-tundra biota? Quat. Sci. Rev. 27, 2473–2483. https://doi.org/10.1016/j.quascirev.2008.09.011.

Ewald, T., Hills, L.V., Tolman, S., Kooyman, B., 2018. Scimitar cat (*Homotherium serum* cope) from southwestern alberta, Canada. Can. J. Earth Sci. 55, 8–17. https://doi.org/10.1139/cjes-2017-0130.

Fancy, S.G., Pank, L.F., Whitten, K.R., Regelin, W.L., 1990. Seasonal movements of caribou in arctic Alaska as determined by satellite. Rangifer 10, 167. https://doi.org/10.7557/2.10.3.850.

Firth, C., Kitchen, A., Shapiro, B., Suchard, M.A., Holmes, E.C., Rambaut, A., 2010. Using time-structured data to estimate evolutionary rates of double-stranded DNA viruses. Mol. Biol. Evol. 27, 2038–2051. https://doi.org/10.1093/molbev/msq088.

Fisher, J.W., 1995. J.W. Bone surface modifications in zooarchaeology. J. Archaeol. Method Theor 2, 7–68.

Flores, D., 1991. Bison ecology and Bison diplomacy: the southern plains from 1800 to 1850. J. Am. Hist. 78, 465. https://doi.org/10.2307/2079530.

Fox-dobbs, K., Leonard, J.A., Koch, P.L., 2008. Pleistocene megafauna from eastern Beringia : paleoecological and paleoenvironmental interpretations of stable carbon and nitrogen isotope and radiocarbon records. Palaeogeogr. Palaeoclimatol. Palaeoecol. 261, 30–46. https://doi.org/10.1016/j.palaeo.2007.12.011.

Froese, D., Stiller, M., Heintzman, P.D., Reyes, A.V., Zazula, G.D., Soares, A.E.R., Meyer, M., Hall, E., Jensen, B.J.L., Arnold, L.J., MacPhee, R.D.E., Shapiro, B., 2017. Fossil and genomic evidence constrains the timing of bison arrival in North America. Proc. Natl. Acad. Sci. Unit. States Am. 114, 3457–3462. https://doi.org/10.1073/pnas.1620754114.

Fuller, B.T., Fuller, J.L., Sage, N.E., Harris, D.A., O'Connell, T.C., Hedges, R.E.M., 2005. Nitrogen balance and $\delta^{15}N$: why you're not what you eat during nutritional stress. Rapid Commun. Mass Spectrom. 19, 2497–2506. https://doi.org/10.1002/rcm.2090.

Fuller, B.T., Richards, M.P., Mays, S.A., 2003. Stable carbon and nitrogen isotope variations in tooth dentine serial sections from Wharram Percy. J. Archaeol. Sci. 30, 1673–1684. https://doi.org/10.1016/S0305-4403(03)00073-6.

Fuller, W.A., 1959. The horns and teeth as indicators of age in bison. J. Wildl. Manag. 23, 342–344. https://doi.org/10.2307/3796894.

Funck, J., Kellam, C., Seaton, T., Wooller, M.J., 2020. Stable isotopic signatures in modern wood bison (*Bison bison athabascae*) hairs as telltale biomarkers of nutritional stress. Can. J. Zool. 98, 505–514. https://doi/10.1139/cjz-2019-0185#.XymTQRNKiek.

Gadbury, C., Todd, L., Jahren, A.H., Amundson, R., 2000. Spatial and temporal variations in the isotopic composition of bison tooth enamel from the Early Holocene Hudson-Meng Bone Bed, Nebraska. Palaeogeogr. Palaeoclimatol. Palaeoecol. 157, 79–93. https://doi.org/10.1016/S0031-0182(99)00151-0.

Gaglioti, B.V., Mann, D.H., Groves, P., Kunz, M.L., Farquharson, L.M., Reanier, R.E., Jones, B.M., Wooller, M.J., 2018. Aeolian stratigraphy describes ice-age paleoenvironments in unglaciated Arctic Alaska. Quat. Sci. Rev. 182, 175–190. https://doi.org/10.1016/j.quascirev.2018.01.002.

Gaglioti, B.V., Mann, D.H., Wooller, M.J., Jones, B.M., Wiles, G.C., Groves, P., Kunz, M.L., Baughman, C.A., Reanier, R.E., 2017. Younger-Dryas cooling and sea-ice feedbacks were prominent features of the Pleistocene-Holocene transition in Arctic Alaska. Quat. Sci. Rev. 169, 330–343. https://doi.org/10.1016/j.quascirev.2017.05.012.

Gigleux, C., Grimes, V., Tütken, T., Knecht, R., Britton, K., 2017. Reconstructing caribou seasonal biogeography in Little Ice Age (late Holocene) Western Alaska using intra-tooth strontium and oxygen isotope analysis. J. Archaeol. Sci. Reports. https://doi.org/10.1016/j.jasrep.2017.10.043.

Glassburn, C.L., Potter, B.A., Clark, J.L., Reuther, J.D., Bruning, D.L., Wooller, M.J., 2018. Strontium and oxygen isotope profiles of sequentially sampled modern Bison (*Bison bison bison*) teeth from interior Alaska as proxies of seasonal mobility. Arctic 71, 185–202.

Glassburn, C.L., Potter, B.A., Clark, J.L., Reuther, J.D., Bruning, D.L., Wooller, M.J., Clark, J.L., Reuther, J.D., Bruning, D.L., Wooller, M.J., 2015. Application of Strontium and Oxygen Isotope Analyses to Sequentially-Sampled Modern bison (Bison bison bison) Teeth from Interior Alaska as a Proxy of Seasonal Mobility. Masters Thesis). Univ. Alaska Fairbanks.

Gomes, L., Augusto, W., Godoy, C., 2006. A review of postfeeding larval dispersal in blowflies : implications for forensic entomology. Naturwissenschaften 93, 207–215. https://doi.org/10.1007/s00114-006-0082-5.

Graham, R.W., Belmecheri, S., Choy, K., Culleton, B.J., Davies, L.J., Froese, D., Heintzman, P.D., Hritz, C., Kapp, J.D., Newsom, L.A., Rawcliffe, R., Saulnier-Talbot, É., Shapiro, B., Wang, Y., Williams, J.W., Wooller, M.J., 2016. Timing and causes of mid-Holocene mammoth extinction on St. Paul Island, Alaska. Proc. Natl. Acad. Sci. Unit. States Am. 201604903 https://doi.org/10.1073/pnas.1604903113.

Green, W.C.H., Rothstein, A., Griswold, J.G., 1993. Weaning and parent-offspring conflict: variation relative to interbirth interval in Bison. Ethology 95, 105–125. https://doi.org/10.1111/j.1439-0310.1993.tb00462.x.

Guthrie, A.R.D., 1966. Bison horn Cores : character choice and systematics. J. Paleontol. 40, 738–740.

Guthrie, R.D., 2001. Origin and causes of the mammoth steppe: a story of cloud cover, woolly mammal tooth pits, buckles, and inside-out Beringia. Quat. Sci. Rev. 20, 549–574. https://doi.org/10.1016/S0277-3791(00)00099-8.

Guthrie, R.D., 1989. Frozen Fauna of Mammoth Steppe: the Story of Blue Babe. University of Chicago Press, Chicago.

Guthrie, R.D., 1970. Bison evolution and zoogeography in north America during the pleistocene. Q. Rev. Biol. 45, 1–15.

Guthrie, R.D., 1968. Paleoecology of the large-mammal community in interior Alaska during the late pleistocene in of the large-mammal community. Am. Midl. Nat. 79, 346–363.

Habran, S., Debier, C., Crocker, D.E., Houser, D.S., Lepoint, G., Bouquegneau, J.M., Das, K., 2010. Assessment of gestation, lactation and fasting on stable isotope ratios in northern elephant seals (*Mirounga angustirostris*). Mar. Mamm. Sci. 26, 880–895. https://doi.org/10.1111/j.1748-7692.2010.00372.x.

Haile, J., Froese, D.G., Macphee, R.D.E., Roberts, R.G., Arnold, L.J., Reyes, A.V., Rasmussen, M., Nielsen, R., Brook, B.W., Robinson, S., Demuro, M., Gilbert, M.T.P., Willerslev, E., Munch, K., Austin, J.J., Cooper, A., Barnes, I., Mo, P., 2009. Ancient DNA reveals late survival of mammoth and horse in interior Alaska. Proc. Natl. Acad. Sci. Unit. States Am. 106, 22352–22357.

Hanson, J.R., 2015. Bison ecology in the Northern plains and a reconstruction of bison patterns for the north Dakota region. Plains Anthropol. 29, 93–113.

Haynes, G., 1980. Paleontological society evidence of carnivore gnawing on pleistocene and recent mammalian bones author (s): gary Haynes published by : paleontological society stable URL. https://www.jstor.org/stable/2400350. Recent mammalian bones. Paleobiology 6.

Heaton, T.H.E., Vogel, J.C., von la Chevallerie, G., Collett, G., 1986. Climatic influence on the isotopic composition of bone nitrogen. Nature 322, 822. https://doi.org/

10.1038/322822a0.
Hedges, R.E.M., Clement, J.G., Thomas, D.L., O'Connell, T.C., 2007. Collagen turnover in the adult femoral mid-shaft modeled from anthropogenic radiocarbon traver measurements. Am. J. Phys. Anthropol. 133, 808–816. https://doi.org/10.1002/ajpa.
Hedges, R.E.M., Stevens, R.E., Richards, M.P., 2004. Bone as a stable isotope archive for local climatic information. Quat. Sci. Rev. 23, 959–965. https://doi.org/10.1016/j.quascirev.2003.06.022.
Heintzman, P.D., Froese, D., Ives, J.W., Soares, A.E.R., Zazula, G.D., Letts, B., Andrews, T.D., Driver, J.C., Hall, E., Gregory Hare, P., Jass, C.N., Mackay, G., Southon, J.R., Stiller, M., Woywitka, R., Suchard, M.A., Shapiro, B., 2016. Bison phylogeography constrains dispersal and viability of the Ice Free Corridor in western Canada. Proc. Natl. Acad. Sci. Unit. States Am. 1–7. https://doi.org/10.1073/pnas.1601077113.
Higgins, P., MacFadden, B.J., 2004. "Amount Effect" recorded in oxygen isotopes of Late Glacial horse (*Equus*) and bison (*Bison*) teeth from the Sonoran and Chihuahuan deserts, southwestern United States. Palaeogeogr. Palaeoclimatol. Palaeoecol. 206, 337–353. https://doi.org/10.1016/j.palaeo.2004.01.011.
Hobbie, J.E., Hobbie, E.A., 2006. ^{15}N in symbiotic fungi and plants estimates nitrogen and carbon flux rates in arctic tundra. Ecology 87, 816–822. https://doi.org/10.1890/0012-9658(2006)87[816:NISFAP]2.0.CO;2.
Hobson, K.A., Alisauskas, R.A.Y.T., Clark, R.G., 1993. Stable-nitrogen isotope enrichment in avian tissues due to fasting and nutritional stress: implications for isotopic analyses of diet. Condor 95, 388–394.
Hobson, K.A., Clark, R.G., 1992. Assessing avian diets using stable isotopes II : factors influencing diet-tissue fractionation. Condor 94, 189–197.
Hoppe, K. a, Koch, P.L., Carlson, R.W., Webb, S.D., 1999. Tracking mammoths and mastodons : reconstruction of migratory behavior using strontium isotope ratios. Geology 27, 439–442. https://doi.org/10.1130/0091-7613(1999)027<0439.
Hoppe, K.A., 2006. Correlation between the oxygen isotope ratio of North American bison teeth and local waters: implication for paleoclimatic reconstructions. Earth Planet Sci. Lett. 244, 408–417. https://doi.org/10.1016/j.epsl.2006.01.062.
Hoppe, K.A., 2004. Late Pleistocene mammoth herd structure, migration patterns, and Clovis hunting strategies inferred from isotopic analyses of multiple death assemblages. Paleobiology 30, 129–145.
Hoppe, K.A., Paytan, A., Chamberlain, P., 2006. Reconstructing grassland vegetation and paleotemperatures using carbon isotope ratios of bison tooth enamel. Geology 34, 649–652. https://doi.org/10.1130/G22745.1.
Hudson, J., 1993. A Carnivore's view of archaeological bone assemblages. In: From Bones to Behavior. The Center for Archaeological Investigations at Southern Illinois University, Carbondale, pp. 273–300.
Hulten, E., 1968. Flora of Alaska and Neighboring Territories. Standford University Press, Standford, California.
Iacumin, P., Bocherens, H., Chaix, L., 2001. C and N stable isotope ratios of fossil cattle keratin horn from Kerma (Sudan): a record of dietary changes. Ital. J. Int. Sci. 14, 41–46.
Jónsson, H., Ginolhac, A., Schubert, M., Johnson, P.L.F., Orlando, L., 2013. MapDamage2.0: fast approximate Bayesian estimates of ancient DNA damage parameters. Bioinformatics 29, 1682–1684. https://doi.org/10.1093/bioinformatics/btt193.
Julien, M., Bocherens, H., Burke, A., Drucker, D.G., Patou-mathis, M., Krotova, O., Péan, S., 2012. Were European steppe bison migratory? $\delta^{18}O$, $\delta^{13}C$ and Sr intra-tooth isotopic variations applied to a palaeoethological reconstruction. Quat. Int. 271, 106–119. https://doi.org/10.1016/j.quaint.2012.06.011.
Kirillova, I.V., Zanina, O.G., Chernova, O.F., Lapteva, E.G., Trofimova, S.S., Lebedev, V.S., Tiunov, A.V., Soares, A.E.R., Shidlovskiy, F.K., Shapiro, B., 2015. An ancient bison from the mouth of the rauchua river (chukotka, Russia). Quat. Res. 84, 232–245. https://doi.org/10.1016/j.yqres.2015.06.003.
Knudson, K.J., Williams, S.R., Osborn, R., Forgey, K., Ryan, P., 2009. The geographic origins of Nasca trophy heads using strontium, oxygen, and carbon isotope data. J. Anthropol. Archaeol. 28, 244–257. https://doi.org/10.1016/j.jaa.2008.10.006.
Koch, P.L., Heisinger, J., Moss, C., Carlson, R.W., Marilyn, L., Koch, P.L., Heisinger, J., Moss, C., Carlson, R.W., Fogel, M.L., Behrensmeyer, A.K., 1995. Isotopic tracking of change in diet and habitat use in african elephants. Science (80-.) 267, 1340–1343.
Koch, P.P.L., Tuross, N., Fogel, M.L., 1997. The effects of sample treatment and diagenesis on the isotopic integrity of carbonate in biogenic hydroxylapatite. J. Archaeol. Sci. 24, 417–429. https://doi.org/10.1006/jasc.1996.0126.
Kootker, L.M., van Lanen, R.J., Kars, H., Davies, G.R., 2016. Strontium isoscapes in The Netherlands. Spatial variations in $^{87}Sr/^{86}Sr$ as a proxy for palaeomobility. J. Archaeol. Sci. Reports 6, 1–13. https://doi.org/10.1016/j.jasrep.2016.01.015.
Kowalczyk, R., Taberlet, P., Coissac, E., Valentini, A., Miquel, C., Kamiński, T., Wójcik, J.M., 2011. Influence of management practices on large herbivore diet-Case of European bison in Białowieza Primeval Forest (Poland). For. Ecol. Manage. 261, 821–828. https://doi.org/10.1016/j.foreco.2010.11.026.
Kristensen, D.K., Kristensen, E., Forchhammer, M.C., Michelsen, A., Schmidt, N.M., 2011. Arctic herbivore diet can be inferred from stable carbon and nitrogen isotopes in C_3 plants, faeces, and wool. Can. J. Zool. 89, 892–899. https://doi.org/10.1139/z11-073.
Lachniet, M.S., Lawson, D.E., Stephen, H., Sloat, A.R., Patterson, W.P., 2016. Isoscapes of d18O and d2H reveal climatic forcings on Alaska and Yukon precipitation. Water Resour. Res. 52, 6575–6586. https://doi.org/10.1002/2016WR019436.Received.
Lambeck, K., Rouby, H., Purcell, A., Sun, Y., Sambridge, M., 2014. Sea level and global ice volumes from the last glacial maximum to the holocene. Proc. Natl. Acad. Sci. U.S.A. 111, 15296–15303. https://doi.org/10.1073/pnas.1411762111.
Larter, N.C., Gates, C.C., 1991. Diet and habitat selection of wood bison in relation to seasonal-changes in forage quantity and quality. Can. J. Zool. 69, 2677–2685. https://doi.org/10.1139/z91-376.
Lee, T.N., Buck, C.L., Barnes, B.M., O'Brien, D.M., 2012. A test of alternative models for increased tissue nitrogen isotope ratios during fasting in hibernating arctic ground squirrels. J. Exp. Biol. 215, 3354–3361. https://doi.org/10.1242/jeb.068528.
Li, H., Durbin, R., 2009. Fast and accurate short read alignment with Burrows-Wheeler transform. Bioinformatics 25, 1754–1760. https://doi.org/10.1093/bioinformatics/btp324.
Lindroth, C.H., 1966. The ground beetles (Carabidae, excl. Cicindellidae) of Canada and Alaska, Part 4. Opusc. Entomol. Suppl. 29, 409–648.
Lisiecki, L.E., Raymo, M.E., 2005. A Pliocene-Pleistocene stack of 57 globally distributed benthic δ18O records. Paleoceanography 20, 1–17. https://doi.org/10.1029/2004PA001071.
Lorenzen, E.D., Nogués-Bravo, D., Orlando, L., Weinstock, J., Binladen, J., Marske, K.A., Ugan, A., Borregaard, M.K., Gilbert, M.T.P., Nielsen, R., Ho, S.Y.W., Goebel, T., Graf, K.E., Byers, D., Stenderup, J.T., Rasmussen, M., Campos, P.F., Leonard, J.A., Koepfli, K.P., Froese, D., Zazula, G., Stafford, T.W., Aaris-Sørensen, K., Batra, P., Haywood, A.M., Singarayer, J.S., Valdes, P.J., Boeskorov, G., Burns, J.A., Davydov, S.P., Haile, J., Jenkins, D.L., Kosintsev, P., Kuznetsova, T., Lai, X., Martin, L.D., McDonald, H.G., Mol, D., Meldgaard, M., Munch, K., Stephan, E., Sablin, M., Sommer, R.S., Sipko, T., Scott, E., Suchard, M.A., Tikhonov, A., Willerslev, R., Wayne, R.K., Cooper, A., Hofreiter, M., Sher, A., Shapiro, B., Rahbek, C., Willerslev, E., 2011. Species-specific responses of Late Quaternary megafauna to climate and humans. Nature 479, 359–364. https://doi.org/10.1038/nature10574.
Lott, D.F., 1971. Sexual and aggressive behavior of American bison (*Bison bison*). In: The Behaviour of Ungulates and its Relation to Management, pp. 382–394.
Lyman, R.L., 1994. Vertebrate Taphonomy. Cambridge University Press, Camrbidge.
Lyman, R.L., 1987. Archaeofaunas and butchery studies: a taphonomic perspective. Adv. Archaeol. Method Theor. 10, 249–337.
Maher, C.R., Byers, J.A., 1987. Age-related changes in reproductive effort of male bison. Behav. Ecol. Sociobiol. 21, 91–96. https://doi.org/10.1007/PL00020232.
Mann, D.H., Groves, P., Kunz, M.L., Reanier, R.E., Gaglioti, B.V., 2013. Ice-age megafauna in Arctic Alaska: extinction, invasion, survival. Quat. Sci. Rev. 70, 91–108. https://doi.org/10.1016/j.quascirev.2013.03.015.
Mann, D.H., Groves, P., Reanier, R.E., Gaglioti, B.V., Kunz, M.L., Shapiro, B., 2015. Life and extinction of megafauna in the ice-age Arctic. Proc. Natl. Acad. Sci. Unit. States Am. 112, 14301–14306. https://doi.org/10.1073/pnas.1516573112.
Männel, T.T., Auerswald, K., Schnyder, H., 2007. Altitudinal gradients of grassland carbon and nitrogen isotope composition are recorded in the hair of grazers. Global Ecol. Biogeogr. 16, 583–592. https://doi.org/10.1111/j.1466-8238.2007.00322.x.
Marcenko, E., Srdoc, D., Golubic, S., Pezdic, J., Head, M.J., 1989. Carbon uptake in aquatic plants deduced from their natural ^{13}C and ^{14}C content. Radiocarbon 31, 785–794. https://doi.org/10.1017/S0033822200012406.
Marsolier-Kergoat, M.C., Palacio, P., Berthonaud, V., Maksud, F., Stafford, T., Begouen, R., Elalouf, J.M., 2015. Hunting the extinct steppe Bison (*Bison priscus*) mitochondrial genome in the trois-freres paleolithic painted cave. PloS One 10, e0128267. https://doi.org/10.1371/journal.pone.0128267.
Martin, J.M., Mead, J.I., Barboza, P.S., 2018. Bison body size and climate change. J. Mammal. 8, 1–11. https://doi.org/10.1002/ece3.4019.
Mekota, A.-M., Grupe, G., Ufer, S., Cuntz, U., 2006. Serial analysis of stable nitrogen and carbon isotopes in hair: monitoring starvation and recovery phase of patients suffering from anorexia nervosa. Rapid Commun. Mass Spectrom. 20, 1604–1610. https://doi.org/10.1002/rcm.
Meyer, H., Schirrmeister, L., Andreev, A., Wagner, D., Hubberten, H.W., Yoshikawa, K., Bobrov, A., Wetterich, S., Opel, T., Kandiano, E., Brown, J., 2010. Lateglacial and Holocene isotopic and environmental history of northern coastal Alaska - results from a buried ice-wedge system at Barrow. Quat. Sci. Rev. 29, 3720–3735. https://doi.org/10.1016/j.quascirev.2010.08.005.
Meyer, M., Kircher, M., 2010. Illumina sequencing library preparation for highly multiplexed target capture and sequencing. Cold Spring Harb. Protoc. https://doi.org/10.1101/pdb.prot5448.
Montgomery, J., Evans, J., Horstwood, M.S.A., 2010. Evidence for long-term averaging of strontium in bovine enamel using TIMS and LA-MC-ICP-MS strontium isotope intra-molar profiles. Environmental archeology. https://doi.org/10.1063/1.2756072.
Moon, T.A., Overeem, I., Druckenmiller, M., Holland, M., Huntington, H., Kling, G., Lovecraft, A.L., Miller, G., Scambos, T., Schädel, C., Schuur, E.A.G., Trochim, E., Wiese, F., Williams, D., Wong, G., 2019. The expanding footprint of rapid arctic change. Earth's Futur 7, 212–218. https://doi.org/10.1029/2018EF001088.
Murray, G.G.R., Wang, F., Harrison, E.M., Paterson, G.K., Mather, A.E., Harris, S.R., Holmes, M.A., Rambaut, A., Welch, J.J., 2016. The effect of genetic structure on molecular dating and tests for temporal signal. Methods Ecol. Evol. 7, 80–89. https://doi.org/10.1111/2041-210X.12466.
Nelson, M.A., Quakenbush, L.T., Mahoney, B.A., Taras, B.D., Wooller, M.J., 2018. Fifty years of Cook Inlet beluga whale feeding ecology from isotopes in bone and teeth. Endanger. Species Res. 36, 77–87. https://doi.org/10.3354/ESR00890.
Paradis, E., Claude, J., Strimmer, K., 2004. APE: analyses of phylogenetics and evolution in R language. Bioinformatics 20, 289–290. https://doi.org/10.1093/bioinformatics/btg412.
Passey, B.H., Robinson, T.F., Ayliffe, L.K., Cerling, T.E., Sponheimer, M., Dearing, M.D.,

Roeder, B.L., Ehleringer, J.R., 2005. Carbon isotope fractionation between diet, breath CO_2, and bioapatite in different mammals. J. Archaeol. Sci. 32, 1459–1470. https://doi.org/10.1016/j.jas.2005.03.015.
Pellegrini, M., Donahue, R.E., Chenery, C., Evans, J., Lee-Thorp, J., Montgomery, J., Mussi, M., 2008. Faunal migration in late-glacial central Italy: implications for human resource exploitation. Rapid Commun. Mass Spectrom. 22, 1714–1726. https://doi.org/10.1002/rcm.3521.
Pellegrini, M., Snoeck, C., 2016. Comparing bioapatite carbonate pre-treatments for isotopic measurements: Part 2 - impact on carbon and oxygen isotope compositions. Chem. Geol. 420, 88–96. https://doi.org/10.1016/j.chemgeo.2015.10.038.
Plumb, G.E., White, P.J., Coughenour, M.B., Wallen, R.L., 2009. Carrying capacity, migration, and dispersal in Yellowstone bison. Biol. Conserv. 142, 2377–2387. https://doi.org/10.1016/j.biocon.2009.05.019.
Post, D.M., 2002. Using stable isotopes to estimate trophic position: models, methods and assumptions. Ecology 83, 703–718.
Post, E., Forchhammer, M.C., 2008. Climate change reduces reproductive success of an Arctic herbivore through trophic mismatch. Philos. Trans. R. Soc. B Biol. Sci. 363, 2369–2375. https://doi.org/10.1098/rstb.2007.2207.
Rabanus-Wallace, M.T., Wooller, M.J., Zazula, G.D., Shute, E., Jahren, A.H., Kosintsev, P., Burns, J.A., Breen, J., Llamas, B., Cooper, A., 2017. Megafaunal isotopes reveal role of increased moisture on rangeland during late Pleistocene extinctions. Nat. Ecol. Evol. 1, 1–5. https://doi.org/10.1038/s41559-017-0125.
Radloff, F.G.T., Mucina, L., Bond, W.J., le Roux, P.J., 2010. Strontium isotope analyses of large herbivore habitat use in the Cape Fynbos region of South Africa. Oecologia 164, 567–578. https://doi.org/10.1007/s00442-010-1731-0.
Rasmussen, S.O., Bigler, M., Blockley, S.P., Blunier, T., Buchardt, S.L., Clausen, H.B., Cvijanovic, I., Dahl-Jensen, D., Johnsen, S.J., Fischer, H., Gkinis, V., Guillevic, M., Hoek, W.Z., Lowe, J.J., Pedro, J.B., Popp, T., Seierstad, I.K., Steffensen, J.P., Svensson, A.M., Vallelonga, P., Vinther, B.M., Walker, M.J.C., Wheatley, J.J., Winstrup, M., 2014. A stratigraphic framework for abrupt climatic changes during the Last Glacial period based on three synchronized Greenland ice-core records: refining and extending the INTIMATE event stratigraphy. Quat. Sci. Rev. 106, 14–28. https://doi.org/10.1016/j.quascirev.2014.09.007.
Reitsema, L.J., Muir, A.B., 2015. Brief communication: growth velocity and weaning $\delta^{15}N$ "dips" during ontogeny in Macaca mulatta. Am. J. Phys. Anthropol. 157, 347–357. https://doi.org/10.1002/ajpa.22713.
Rivals, F., Mihlbachler, M.C., Solounias, N., Mol, D., Semprebon, G.M., de Vos, J., Kalthoff, D.C., 2010. Palaeoecology of the Mammoth Steppe fauna from the late Pleistocene of the North Sea and Alaska: separating species preferences from geographic influence in paleoecological dental wear analysis. Palaeogeogr. Palaeoclimatol. Palaeoecol. 286, 42–54. https://doi.org/10.1016/j.palaeo.2009.12.002.
Rivals, F., Solounias, N., Mihlbachler, M.C., 2007. Evidence for geographic variation in the diets of late Pleistocene and early Holocene Bison in North America, and differences from the diets of recent Bison. Quat. Res. 68, 338–346. https://doi.org/10.1016/j.yqres.2007.07.012.
Rode, K.D., Stricker, C.A., Erlenbach, J., Robbins, C.T., Cherry, S.G., Newsome, S.D., Cutting, A., Jensen, S., Stenhouse, G., Brooks, M., Hash, A., Nicassio, N., 2016. Isotopic incorporation and the effects of fasting and dietary lipid content on isotopic discrimination in large carnivorous mammals. Physiol. Biochem. Zool. 89, 182–197. https://doi.org/10.1086/686490.
Rode, K.D., Wilson, R.R., Douglas, D.C., Muhlenbruch, V., Atwood, T.C., Regehr, E.V., Richardson, E.S., Pilfold, N.W., Derocher, A.E., Durner, G.M., Stirling, I., Amstrup, S.C., St Martin, M., Pagano, A.M., Simac, K., 2018. Spring fasting behavior in a marine apex predator provides an index of ecosystem productivity. Global Change Biol. 24, 410–423. https://doi.org/10.1111/gcb.13933.
Saarinen, J.J., Eronen, J.T., Fortelius, M., Seppa, H., Lister, A., 2016. Patterns of body mass and diet of large ungulates from Middle and Late Pleistocene of Western Europe and their connections with vegetation openness. Paleontol. Electron. 1–58.
Scherler, L., Tütken, T., Becker, D., 2014. Carbon and oxygen stable isotope compositions of late Pleistocene mammal teeth from dolines of Ajoie (Northwestern Switzerland). Quat. Res. 82, 378–387. https://doi.org/10.1016/j.yqres.2014.05.004.
Schmieder, R., Edwards, R., 2011. Quality control and preprocessing of metagenomic datasets. Bioinformatics 27, 863–864. https://doi.org/10.1093/bioinformatics/btr026.
Schoeninger, M.J., DeNiro, M.J., 1984. Nitrogen and carbon isotopic composition of bone collagen from marine and terrestrial animals. Geochem. Cosmochim. Acta 48, 625–639. https://doi.org/10.1016/0016-7037(84)90091-7.
Schubert, B.W., 2010. Late Quaternary chronology and extinction of North American giant short-faced bears (*Arctodus simus*). Quat. Int. 217, 188–194. https://doi.org/10.1016/j.quaint.2009.11.010.
Schwartz-Narbonnea, R., Longstaffea, F.J., Kardynalb, K.J., Druckenmiller, P., Hobson, K.A., Jasse, C.N., Metcalfe, J.Z., Zazula, J.Z., 2019. Reframing the mammoth steppe: insights from analysis of isotopic niches. Quat. Sci. Rev. 215, 1–21. https://doi.org/10.1016/j.quascirev.2019.04.025.
Shapiro, B., Cooper, A., 2003. Beringia as an ice age genetic museum. Quat. Res. 60, 94–100. https://doi.org/10.1016/S0033-5894(03)00009-7.
Shapiro, B., Ho, S.Y.W., Drummond, A.J., Suchard, M.A., Pybus, O.G., Rambaut, A., 2011. A bayesian phylogenetic method to estimate unknown sequence ages. Mol. Biol. Evol. 28, 879–887. https://doi.org/10.1093/molbev/msq262.
Shapiro, B., Pybus, O.G., Gilbert, M.T.P., Barnes, I., Baryshnikov, G.F., Burns, J.A., Davydov, S., 2004. Rise and fall of the beringian steppe Bison. Science (80- 306, 1561–1565. https://doi.org/10.1126/science.1101074.
Sharma, S., Couturier, S., Côté, S.D., 2009. Impacts of climate change on the seasonal distribution of migratory caribou. Global Change Biol. 15, 2549–2562. https://doi.org/10.1111/j.1365-2486.2009.01945.x.
Smith, K.G.V., 1986. A Manual of Forensic Entomology. Trustees of the British Museum, Oxford.
Soper, J.D., 1941. History, range and home life of the northern Bison. Ecol. Monogr. 11, 347–412. https://doi.org/10.2307/1943298.
Sorkin, B., 2006. Ecomorphology of the giant short-faced bears Agriotherium and Arctodus. Hist. Biol. 18, 1–20. https://doi.org/10.1080/08912960500476366.
Stevens, R.E., Balasse, M., O'Connell, T.C., 2011. Intra-tooth oxygen isotope variation in a known population of red deer: implications for past climate and seasonality reconstructions. Palaeogeogr. Palaeoclimatol. Palaeoecol. 301, 64–74. https://doi.org/10.1016/j.palaeo.2010.12.021.
Stevens, R.E., Hedges, R.E., 2004. Carbon and nitrogen stable isotope analysis of northwest European horse bone and tooth collagen, 40,000BP–present: palaeoclimatic interpretations. Quat. Sci. Rev. 23, 977–991. https://doi.org/10.1016/j.quascirev.2003.06.024.
Stevens, R.E., Lister, M., Hedges, R.E.M., 2006. Predicting diet, trophic level and paleoecology from bone stable isotope analysis: a comparative study of five red deer populations. Oecologia 149, 12–21. https://doi.org/10.1007/s00442-006-0416-1.
Stuiver, M., Reimer, P.J., Reimer, R.W., 2019. Calib 7.1.
Taylor, R.E., Hare, P.E., Prior, C.A., Kirner, D.L., Want, L., Burkyi, R.R., 1995. Radiocarbon dating of biochemically characterized hair. Radiocarbon 37, 319–330. https://doi.org/10.1017/S0033822200030794.
Van Geel, B., Protopopov, A., Bull, I., Duijm, E., Gill, F., Lammers, Y., Nieman, A., Rudaya, N., Trofimova, S., Tikhonov, A.N., Vos, R., Zhilich, S., Gravendeel, B., 2014. Multiproxy diet analysis of the last meal of an early Holocene Yakutian bison. J. Quat. Sci. 29, 261–268. https://doi.org/10.1002/jqs.2698.
Velivetskaya, T.A., Smirnov, N.G., Kiyashko, S.I., Ignatiev, A.V., Ulitko, A.I., 2016. Resolution-enhanced stable isotope profiles within the complete tooth rows of Late Pleistocene bisons (Middle Urals, Russia) as a record of their individual development and environmental changes. Quat. Int. 400, 212–226. https://doi.org/10.1016/j.quaint.2014.12.011.
Verkouteren, R.M., Klinedinst, D.B., 2004. Value Assignment and Uncertainty Estimation of Selected Light Stable Isotope Reference Materials: RMs 8543-8545, RMs 8562-8564, and RM 8566. National Institute of Standards and Technology Special Publication.
Viner, S., Evans, J., Albarella, U., Parker Pearson, M., 2010. Cattle mobility in prehistoric britain: strontium isotope analysis of cattle teeth from durrington walls (wiltshire, britain). J. Archaeol. Sci. 37, 2812–2820. https://doi.org/10.1016/j.jas.2010.06.017.
Voigt, C.C., Matt, F., 2004. Nitrogen stress causes unpredictable enrichments of ^{15}N in two nectar-feeding bat species. J. Exp. Biol. 207, 1741–1748. https://doi.org/10.1242/jeb.00929.
Waggoner, V., Hinkes, M., 1986. Summer and fall browse utilization by an alaskan Bison herd. J. Wildl. Manag. 50, 322–324.
Warren, J., Anderson, G.S., 2013. The development of Protophormia terraenovae (Robineau-Desvoidy) at constant temperatures and its minimum temperature threshold. Forensic Sci. Int. 233, 374–379. https://doi.org/10.1016/j.forsciint.2013.10.012.
Widga, C., Walker, J.D., Stockli, L.D., 2010. Middle Holocene Bison diet and mobility in the eastern Great Plains (USA) based on ^{13}C, ^{18}O, and $^{87}Sr/^{86}Sr$ analyses of tooth enamel carbonate. Quat. Res. 73, 449–463. https://doi.org/10.1016/j.yqres.2009.12.001.
Wiener, D.J., Wiedemar, N., Welle, M.M., Drögemüller, C., 2015. Novel features of the prenatal horn bud development in cattle (*Bos taurus*). PloS One 10, 1–13. https://doi.org/10.1371/journal.pone.0127691.
Willerslev, E., Davison, J., Moora, M., Zobel, M., Coissac, E., Edwards, M.E., Lorenzen, E.D., Vestergård, M., Gussarova, G., Haile, J., Craine, J., Gielly, L., Boessenkool, S., Epp, L.S., Pearman, P.B., Cheddadi, R., Murray, D., Bråthen, K.A., Yoccoz, N., Binney, H., Cruaud, C., Wincker, P., Goslar, T., Alsos, I.G., Bellemain, E., Brysting, A.K., Elven, R., Sønstebø, J.H., Murton, J., Sher, A., Rasmussen, M., Rønn, R., Mourier, T., Cooper, A., Austin, J., Möller, P., Froese, D., Zazula, G., Pompanon, F., Rioux, D., Niderkorn, V., Tikhonov, A., Savvinov, G., Roberts, R.G., Macphee, R.D.E., Gilbert, M.T.P., Kjær, K.H., Orlando, L., Brochmann, C., Taberlet, P., 2014. Fifty thousand years of Arctic vegetation and megafaunal diet. Nature 506, 47–51. https://doi.org/10.1038/nature12921.
Wooller, M.J., Zazula, G.D., Edwards, M., Froese, D.G., Boone, R.D., Parker, C., Bennett, B., 2007. Stable carbon isotope compositions of Eastern Beringian grasses and sedges: investigating their potential as paleoenvironmental indicators. Arctic Antarct. Alpine Res. 39, 318–331. https://doi.org/10.1657/1523-0430(2007)39[318:SCICOE]2.0.CO;2.
Zazula, G.D., Hall, E., Hare, P.G., Thomas, C., Mathewes, R., La Farge, C., Martel, A.L., Heintzman, P.D., Shapiro, B., 2017. A middle holocene steppe bison and paleoenvironments from the Versleuce Meadows, Whitehorse, Yukon, Canada. Can. J.

Earth Sci. 54, 1138–1152. https://doi.org/10.1139/cjes-2017-0100.
Zazula, G.D., MacKay, G., Andrews, T.D., Shapiro, B., Letts, B., Brock, F., 2009. A late Pleistocene steppe bison (*Bison priscus*) partial carcass from Tsiigehtchic, Northwest Territories, Canada. Quat. Sci. Rev. 28, 2734–2742. https://doi.org/10.1016/j.quascirev.2009.06.012.
Zazzo, A., Bendrey, R., Vella, D., Moloney, A.P., Monahan, F.J., Schmidt, O., 2012. A refined sampling strategy for intra-tooth stable isotope analysis of mammalian enamel. Geochem. Cosmochim. Acta 84, 1–13. https://doi.org/10.1016/j.gca.2012.01.012.
Zimov, A.S.A., Chuprynin, V.I., Oreshko, A.P., Iii, F.S.C., Reynolds, J.F., 2011. Steppe-tundra Transition : a herbivore-driven biome shift at the end of the pleistocene. Am. Soc. Nat. 146, 765–794. https://doi.org/10.1086/285824.
Zimov, S.A., Zimov, N.S., Tikhonov, A.N., Chapin, I.S., 2012. Mammoth steppe: a high-productivity phenomenon. Quat. Sci. Rev. 57, 26–45. https://doi.org/10.1016/j.quascirev.2012.10.005.